

# Energy return on investment analysis of the 2035 Belgian energy system

Jonathan Dumas<sup>a,\*</sup>, Antoine Dubois<sup>a</sup>, Paolo Thiran<sup>b</sup>, Pierre Jacques<sup>b</sup>, Francesco Contino<sup>b</sup>, Bertrand Cornélusse<sup>a</sup>, Gauthier Limpens<sup>b</sup>

<sup>a</sup>Liege University, Departments of Computer Science and Electrical Engineering, Belgium

<sup>b</sup>Catholic University of Louvain, Institute of Mechanics, Materials and Civil Engineering, Belgium

---

## Abstract

Planning the defossilization of energy systems by facilitating high penetration of renewables and maintaining access to abundant and affordable primary energy resources is a nontrivial multi-objective problem encompassing economic, technical, environmental, and social aspects. However, so far, most long-term policies to decrease the carbon footprint of our societies consider the cost of the system as the leading indicator in the energy system models. To address this gap, we developed a new approach by adding the *energy return on investment* (EROI) in a whole-energy system model. We built the database with all EROI technologies and resources considered while keeping the core components of the model: open access, multi-energy carriers, short computational time, and accounting for all the energy sectors. This novel model is applied to the Belgian energy system in 2035 for several greenhouse gas emissions targets. However, moving away from fossil-based to carbon-neutral energy systems raises the issue of the uncertainty of low-carbon technologies and resource data. Thus, we conduct a global sensitivity analysis to identify the main parameters driving the variations in the EROI of the system.

In this case study, the main results are threefold: (i) the EROI of the system decreases from 8.9 to 3.9 when greenhouse gas emissions are reduced by 5; (ii) the renewable fuels - mainly imported renewable gas - represent the largest share of the system primary energy mix due to the lack of endogenous renewable resources such as wind and solar; (iii) in the sensitivity analysis, the renewable fuels drive 67% of the variation of the EROI of the system for low greenhouse gas emissions scenarios. The decrease in the EROI of the system raises questions about meeting the climate targets without adverse socio-economic impact. Thus, accounting for other criteria in energy planning models that nuance the cost-based results is essential to guide policy-makers in addressing the challenges of the energy transition. Still, this study is a first step in promoting the EROI indicator of a whole-energy system. Several extensions, such as considering various interconnected countries to better benefit from domestic renewable resources or refining the data on renewable fuels and reducing their uncertainties, will motivate future works.

**Keywords:** EROI; energy transition; energy system modelling; sensitivity analysis; EnergyScope TD; polynomial chaos expansion; sectors coupling.

---

## 1. Introduction

To limit climate change and achieve the ambitious targets prescribed by the Intergovernmental Panel on Climate Change [1], the transition toward a carbon-free society goes through an inevitable increase in the share of renewable generation in the energy mix. Integrating these new energy resources and technologies will lead to profound structural changes in energy systems, such as an increasing need for storage and radical electrification of the heating and mobility sectors. Therefore, energy planners face the double challenge of transitioning towards more sustainable fossil-free energy systems, including high penetration of renewables, while preserving access to abundant and affordable primary energy resources. In the literature, a large variety of energy models exists. Limpens et al. [2] has conducted an extensive review of 53 energy models and tools. They all consider a cost-based objective function with sometimes a greenhouse gas emissions target. However, designing an optimal energy system is a multi-objective problem as it encompasses economic, technical, environmental, and social aspects. Thus, new flexible and

tion of the heating and mobility sectors. Therefore, energy planners face the double challenge of transitioning towards more sustainable fossil-free energy systems, including high penetration of renewables, while preserving access to abundant and affordable primary energy resources. In the literature, a large variety of energy models exists. Limpens et al. [2] has conducted an extensive review of 53 energy models and tools. They all consider a cost-based objective function with sometimes a greenhouse gas emissions target. However, designing an optimal energy system is a multi-objective problem as it encompasses economic, technical, environmental, and social aspects. Thus, new flexible and

---

\*Corresponding author

Email address: [jdumas@uliege.be](mailto:jdumas@uliege.be) (Jonathan Dumas)

open-source optimization modeling tools are required to capture the increasing complexity of future energy systems.

This study addresses this issue by considering a comprehensive indicator: the *energy return on investment* (EROI). It better encompasses the technical and social challenges of energy transition than the cost. The field of net energy analysis first came to attention during the 1970s oil crises to assess how much energy is provided to society [3]. Then, various metrics have been introduced in the past few decades, including the energy profit ratio, energy gain, energy payback, and the most well-known, the EROI. Expressed as a ratio [4], the EROI is the amount of helpful energy yielded from each unit of energy input to obtain that energy. The lower the EROI of an energy source, the more input energy is required to produce the output energy, which results in less net energy available for consumption. Thus, the EROI can be understood as the ease with which the energy system can extract energy sources and transform them into a form beneficial to society. The work of Mulder and Hagens [5] established a theoretical framework for EROI analysis that encompasses the various methodologies in the literature.

Access to abundant and affordable primary energy resources has been recognized as an essential element for the prosperity of human societies, and the concept of EROI is commonly used to measure their quality. The literature about EROI is abundant and, without being exhaustive, concerns three main fields of research: (1) the link between EROI and societal well-being; (2) estimation of the EROI of an energy resource or technology; (3) estimation of the EROI at the level of an economy or a society.

The potential connections between societal well-being and net energy availability are investigated by Lambert et al. [6]. The results for a large sample of countries point out that the estimated societal EROI is correlated with the Human Development Index (HDI), which is a standard living indicator. However, for a few countries with a high level of development, HDI above 0.75, there is a saturation point where increasing the EROI above 20 is not associated with further improvement in society. In addition, the relationship between EROI and HDI is non-linear as the HDI increases less and less rapidly with societal EROI.

The characteristics of the primary energy sources, including the EROI of each fuel, are investigated by Hall et al. [7]. They conclude that: (i) the EROI of critical fuels, such as oil and gas, is declining; (ii) most renewable and non-conventional energy alternatives have substantially lower EROI values than traditional conventional

fossil fuels. Another more recent study [8] estimates the EROI of fossil fuels at both primary and final energy stages. However, their results suggest that the current EROI of fossil fuels may not differ from the EROI of renewables, which illustrates the difficulty of adequately assessing the EROI of resources or technologies.

Several attempts to determine a lower bound of the societal EROI have been performed over the past few years. However, the estimation differs from one contribution to another. The study of Hall et al. [9] calculates a lower bound around 5 of the societal EROI below which a prosperous lifestyle would not be sustainable. The study of Court [10] estimates that the minimum sustainable societal EROI has declined from 20 in 1900 to 6 in 1970 to remain constant so far. Brandt [11] estimates a minimum societal EROI of around 5 by using a simple template economy with four sectors and inputs for each sector defined at an order-of-magnitude level using data for the US.

Finally, a few studies have attempted to estimate the societal EROI at a country or world level. The work of Dupont et al. [12] provides an estimate of the societal EROI using a simple macroeconomic model with two sectors, an energy sector and a final sector aggregating the rest of the economy. In addition, they use the net energy ratio, which is more comprehensive than the EROI, to assess the energy embodied in the intermediate and capital consumptions of the entire economy. The model estimates a net worldwide EROI of 8.5 for 2018, and the sensitivity analysis performed on the model parameters demonstrates the robustness of the model. However, their model focuses only on the actual system EROI and does not assess how it would evolve with a transition towards an energy system based mainly on intermittent renewable energy sources to meet the IPCC targets.

These papers illustrate the difficulty of assessing the EROI of a given resource, technology, or society. However, they depict the key elements which have contributed to the increased attention paid to the EROI research field: (1) the EROI of the essential fuels, in particular fossil fuels, has been declining due to the depletion of finite resources [9, 13]; (2) the estimated EROI ratios for renewable energy sources and conventional fossil fuels are often controversial and vary significantly depending on the adopted methodology [7, 8]. This matter raises concerns that the renewables-led energy transition required to meet climate targets may have adverse socioeconomic impacts [14]; (3) the EROI captures the efficiency of energy conversion technologies and provides some macro-economic perspective because of its link to the well-being of society [6].

We provide two reasons to assess the EROI of a

whole-energy system instead of a set of technologies and resources or only a given system sector, such as the electricity grid. First, it is not relevant to compare the EROI of renewable resources or technologies independently. For instance, solar and wind energies are intermittent and stochastic. Gas and nuclear power plants are adjustable and can meet fluctuating demand. Thus, comparing the EROI of solar *vs.* nuclear without taking into account storage systems and other assets to balance the system is not pertinent. Second, a whole-energy system comprises several sectors (mobility, heat, electricity, industry) that use several technologies and resources that can be imported or extracted. These resources are transported, stored, and converted by energy conversion technologies to supply end-use demands such as electricity, transport, heating, and the production of goods. Assessing an energy system as a whole opens the opportunity for the full deployment of synergies and generates unexpected results [15]. Thus, the EROI of the system cannot be the sum of the EROI of each of its components.

The literature comprises a large variety of energy models (optimization and simulation), and we refer the reader to the reviews proposed by Limpens et al. [2], Borasio and Moret [16] which compare models with the following features: open-source, with a monthly to hourly time resolution, and modeling mobility and heat supply besides the electricity sector. While there are many studies devoted to planning a whole-energy system based on the cost indicator, those that consider the EROI are much rarer. MEDEAS-World [17, 18] a global, one-region energy-economy-environment model, is one of the few models which take into account the societal EROI evolution. MEDEAS is a policy-simulation dynamic-recursive model that has been designed by applying System Dynamics. The EROI of the system is estimated, based on a detailed review of the life cycle analyses of the different energy sources, including the ancillary structures required to handle the intermittency of renewable energies. For 2015, using aggregated data at the world level, the model estimated an EROI of the system of 12. Then, the results reveal a fast transition to reach a 100% renewable electric system by 2060, consistent with the Green Growth narrative<sup>1</sup>, which could decrease the EROI of the system from 12 to 3 by the mid-century.

In this present work, we concentrate on optimization models that reveal optimal configurations over many available options and degrees of freedom. They are suit-

able for analyzing complex systems, where many combined alternatives need to be explored. However, the study Borasio and Moret [16] illustrates that there is no perfect energy model capable of addressing all case studies and research topics. It is improbable that a single modeling framework will ever be able to capture all the relevant and interlinked dynamics of the energy transition, which is a complicated and interdisciplinary challenge [15]. Various models can answer different research questions and can be complementary. However, selecting a particular model among the wide range of available energy models is a difficult task. Thus, building on existing and consolidated frameworks can be advantageous over developing new case-specific models from scratch.

We decided to use EnergyScope Typical Days (EnergyScope TD) [2], an open-source model for the strategic energy planning of urban and regional energy systems. Compared to other existing energy models, which are often proprietary, computationally expensive, and primarily focused on the electricity sector, EnergyScope TD optimizes both the investment and operating strategy of an entire energy system, including electricity, heating, mobility, and the non-energy demand<sup>2</sup> (NED). Therefore, the EnergyScope TD model offers several benefits compared to other modeling approaches and can easily be extended to include new indicators such as the EROI. In the following, we focus on the recent works related to EnergyScope TD.

### 1.1. Related work

A first attempt to consider the EROI to investigate the Belgian energy system is conducted by Limpens and Jeanmart [20]. The study focuses on the energy storage mix required to allow the penetration of a high share of renewable energy. A simplified hourly-based model optimizes the renewable energy and storage assets by maximizing the EROI while respecting energy balance constraints. The results indicate that depending on the renewable energy deployment and the nuclear share in the energy mix, the system EROI ranges from 5 to 10.5. However, one of the main limitations of this study relies on the model, which is not a whole-energy system. This issue is addressed with EnergyScope TD by Limpens et al. [2], a more advanced model of the Belgian energy system.

<sup>1</sup>It is an alternative paradigm usually assumed to avoid the adverse impacts on human societies of the global environmental change.

<sup>2</sup>The NED comprises energy products used as raw materials in the different sectors, not consumed as a fuel or transformed into another fuel [19]. In the case of Belgium, it amounts to 20% of the total energy demand and 10% of the world final energy consumption.

First, the EnergyScope TD model was applied to analyze the 2035 Belgian energy system for different carbon emission targets. The results estimate a lack of endogenous resources in Belgium of 275.6 [TWh/y], amounting to 30-40% of the primary energy. Several recommendations are proposed to obtain additional potential such as importing renewable fuels and electricity or deploying geothermal energy. In this study, a mix of solutions is the most cost-effective for reaching low carbon emissions.

Second, a further step is achieved by considering the importance of renewable fuels in a low-carbon energy system [21]. This study performs the uncertainty quantification on a whole-energy model by considering the total annualized cost of the system in the objective of EnergyScope TD. The polynomial chaos expansion method is implemented to perform the sensitivity analysis and highlights the influence of the critical parameters on the cost of the system. The results indicate: (i) when considering uncertain parameters, the average value of the system cost is 17% higher at carbon neutrality than in a deterministic setting; (ii) the standard deviation of the cost increases when decreasing the GHG emissions; (iii) renewable fuels are the primary driver of the system cost uncertainty with 53% of the cost variation.

Finally, a preliminary implementation of a multi-criteria approach in the EnergyScope TD model, which is currently a single objective model, is proposed by Muylldermans and Nève [22]. Given the challenges associated with the energy transition, it allows for assessing a system including economic, environmental, technical, and social aspects. The case study is the 2035 Belgian energy system. The analysis emphasizes the environmental impacts of the energy system according to the weight associated with each criterion in the objective function: the total system cost, EROI, and global warming potential. They conclude that considering multiple criteria leads to a more nuanced and robust solution than a single criterion approach. However, this work is introductory, and the results must be consolidated with a more extensive analysis. In addition, it does not: (i) consider several greenhouse gas emissions scenarios; (ii) assess the uncertainty of the model input parameters. Nevertheless, it paves the way for this paper.

## 1.2. Research gaps and scientific contributions

The research gaps motivating this paper are three-fold:

1. To the best of our knowledge, many studies have considered the EROI a research topic but are focused on specific technologies and are usually con-

ducted in economic and social sciences. In the energy sector, most studies use the cost as an indicator to investigate the transition of a whole energy system. However, only a few preliminary analyses [20, 17, 22] considered the EROI;

2. There is no consolidated EROI dataset for all technologies and resources of a whole-energy system;
3. There is no comparison of the system EROI, accounting for parameters uncertainties, to the deterministic cost-optimum situation.

With these research gaps in mind, the main contributions of this paper, built on the previous studies [20, 2, 21, 22], are four-fold:

1. Conduct an extensive study of the EROI of the Belgian energy transition for several GHG emissions targets. Then, compare the results when considering the cost;
2. Provide a transparent and collaborative database of the EROI of all technologies and resources of a whole-energy system;
3. Assess the impact of uncertain parameters, compared to deterministic analysis, on system EROI using a long-term energy planning model.
4. Emphasize the role of renewable fuels in the purpose of decreasing the GHG emissions;

In addition to these contributions, this study also provides open access to the code repository<sup>3</sup> and the latest documentation<sup>4</sup> to help the community reproduce the experiments. Table 1 presents a comparison of the present study to several state-of-the-art papers analyzing energy transition systems. [Appendix A](#) provides the justifications.

We hope the present work provides decision-makers with insightful guidelines to answer the following questions: (i) What are the main changes in the transition of an energy system when considering the EROI compared to the total system cost? (ii) To what extent should uncertainties be considered when planning a low-carbon energy system based on the maximization of EROI? Furthermore, which are the key parameters that drive the system EROI uncertainty? (iii) Given the limited availability of local renewables in Belgium, what solutions of the Mix scenario presented by Limpens et al. [23], such as electrification, nuclear energy, and import of synthetic fuels, would most affect the variation of the system EROI?

Criteria	[24]	[25]	[26]	[27]	[28]	[23, 21]	Study
Authors	EU	FPB	EV	ELIA	RTE	UCL	UCL-ULG
Multi-sectors	✓	✗	✓	✗	✗	✓	✓
Multi-scenario	✗	~	✓	✓	✓	✓	✓
Model	PRIMES [29]	CSG [30]	TIMES [31]	Antares [32, 33]	EnergyScope TD [2]		
EROI	✗	✗	✗	✗	✗	✗	✓
Sensitivity analysis	✗	✗	✗	✗	✗	✓	✓
Open dataset	✗	✗	~	~	✗	✓	✓
Open-access code	✗	✗	✗	✓	✓	✓	✓

Table 1: The contributions of the present study are compared to several state-of-the-art studies about energy system transition. The justifications are provided in [Appendix A](#).

✓: criteria fully satisfied, ~: criteria partially satisfied, ✗: criteria not satisfied. Multi-sectors: whole-energy system considered; Multi-scenario: several scenarios of GHG emissions; EROI: EROI-based objective function; Sensitivity analysis: uncertainty analysis of the model parameters; Open dataset: the data used are in open-access; Open-access code: the code used to conduct the experiments is in open-access. Abbreviations: European Commission (EU), Federal Plan Bureau (FPB), EnergyVille (EV), France’s transmission system operator (RTE), Belgium’s transmission system operator (ELIA), UCLouvain (UCL), ULiège (ULG), Price-Induced Market Equilibrium System (PRIMES), Crystal Super Grid (CSG), The Integrated MARKAL-EFOM System (TIMES).

### 1.3. Organization

Figure 1 depicts the paper skeleton, which is organized as follows. Section 2 presents the EROI definition used in this study and provides the succinct formulation of the EnergyScope TD model with the main assumptions. Section 3 provides the real-world case study of the Belgian energy system in 2035, and Section 4 investigates its EROI evolution for several GHG emissions targets. Section 5 presents the results of the EROI sensitivity analysis, and Section 6 points out the model and methodology limitations. Finally, Section 7 outlines the main findings and proposes ideas for further work. [Appendix A](#) presents the justifications of the comparison conducted in Table 1. [Appendix B](#) provides the methodology to derive the final energy consumption from the simulation results in EnergyScope TD. Finally, [Appendix C](#) and [Appendix D](#) give additional results of the EROI study of the Belgian energy system in 2035 and the sensitivity analysis, respectively.

## 2. Methodology

This section presents the EROI definition used in this study and details the main assumptions of the model, including the EROI-based objective function.

The EnergyScope TD complete formulation, the documentation of the model, and the input data are described in Limpens et al. [2, Appendix C. Supplementary material], and the code repository with the data is open-access.

### 2.1. EROI definition

This study considers the EROI defined at the final energy stage

$$\text{EROI}_{\text{fin}} = \frac{\text{Gross energy produced}}{\text{Energy invested}} = \frac{E_{\text{out}}}{E_{\text{in}}}. \quad (1)$$

The motivation of this definition is that energy enters the productive economy at the final energy stage. Figure 2 depicts the differences between primary energy, final energy consumed, and end-use demand with the concept of energy cascade. It illustrates the EROI of the system at the final stage.

In (1),  $E_{\text{out}}$  is computed at the final stage, *i.e.*, the quantity of gasoline or electricity required by cars and trains, the heat produced for warming buildings, or the electricity delivered to households and companies.  $E_{\text{in}}$  is also measured in terms of final energy. It is composed of: (1) the energy required for building all the infrastructure of the energy system, from the cradle to the grave; (2) the energy used for operating the energy system; (3) the energy employed for building and operating the infrastructure.

<sup>3</sup><https://github.com/energyscope/EnergyScope>

<sup>4</sup><https://energyscope-td.readthedocs.io/en/master/>

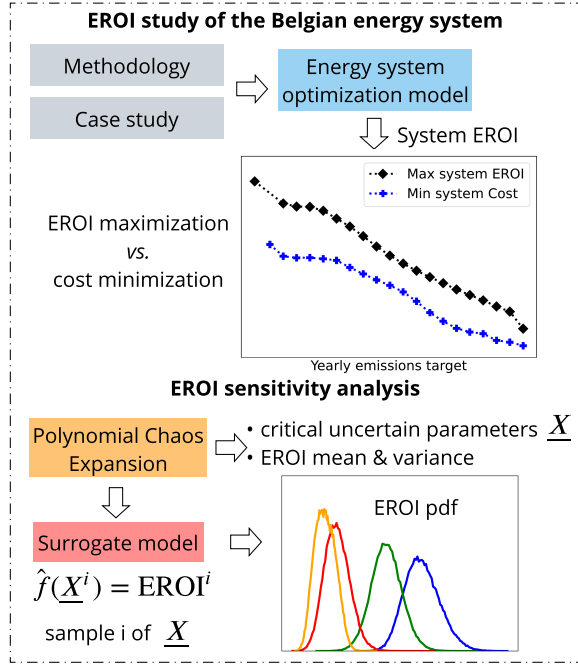


Figure 1: Paper skeleton with the main contributions. The energy system optimization model EnergyScope TD is used to assess the EROI of the Belgian energy system for several GHG emissions targets. Then, an EROI sensitivity analysis identifies the critical uncertain parameters  $\underline{X} \in \mathbb{R}^N$  and estimates the EROI probability density functions using the surrogate model  $\hat{f}$ .

## 2.2. EROI formulation of EnergyScope TD

This study uses the open-source energy system optimization model EnergyScope TD [2], built on previous works [34, 35]. EnergyScope TD is a linear programming (LP), multi-sector, and multi-carrier model for the regional whole-energy system such as a country. This model has been validated for the 2035 Belgian whole-energy system by Limpens et al. [23], which is the case study of interest. Furthermore, the model has been used for several regions<sup>5</sup> including Italy [16], Spain [36], Switzerland [34], and Europe-26 [37]. In addition, Thiran et al. [38] developed a multi-regional version, called EnergyScope Multi-Cell, which was applied to Western Europe [39] and Italy [40].

EnergyScope TD represents the heating, mobility, and electricity sectors with the same level of detail. The main characteristics are: (i) satisfying the system end-use demand (EUD) instead of final energy consumption (FEC). The system EUD is composed of electricity, heat, transport, and non-energy demands. For instance,

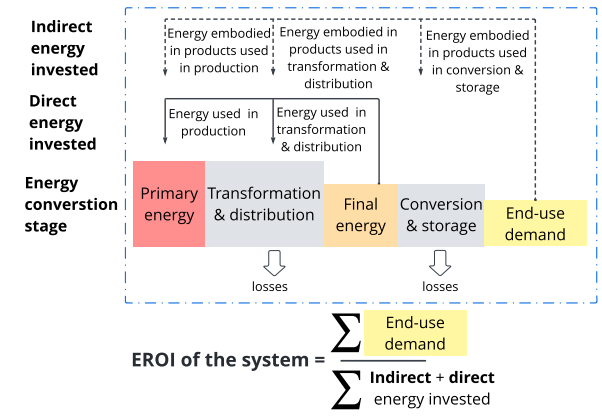


Figure 2: The energy cascade illustrates the system EROI at the final stage considered in this study. This Figure was adapted from Brockway et al. [8].

passenger mobility is defined in passenger kilometers per year rather than in a certain amount of gasoline to fuel cars or electricity to power trains; (ii) optimizing the system design and operation by minimizing its overall cost. In this study, the objective function is modified to maximize  $\text{EROI}_{\text{fin}}$ ; (iii) an hourly resolution which makes the model suitable for analyzing the integration of intermittent renewable energy resources and storage; (iv) the country is modeled as a single node where transmissions within the country are not considered. The demands are balanced by the generations without considering the flows between the producers and the consumers; (v) a short computational time, typically a few minutes, due to the use of typical days, and a rebuilt method to represent a year with an hourly resolution.

The model uses fixed EUD as input parameters where the EUD is related to the numerator in the  $\text{EROI}_{\text{fin}}$  definition (1). Therefore, maximizing the system EROI is equivalent to minimizing the denominator: the energy invested  $E_m$ . Thus, the model optimizes the energy invested and the operational strategies to minimize the total annual system energy invested  $\mathbf{E}_{\text{in,tot}}$  given: (1) the exogenous EUD in electricity, heat, non-energy demand, and mobility; (2) the availability and the energy invested in the operation of the resources (RES) such as natural gas, wind and solar energies, biomass or renewable fuels; (3) the efficiency and the energy invested in the construction of technologies (TECH) such as power plants, wind turbine, heat pumps, or cars. The objective function to minimize is

$$\min \mathbf{E}_{\text{in,tot}} = \sum_{j \in \text{TECH}} \frac{\mathbf{E}_{\text{constr}}(j)}{\text{lifetime}(j)} + \sum_{i \in \text{RES}} \mathbf{E}_{\text{op}}(i), \quad (2)$$

<sup>5</sup><https://energyscope.readthedocs.io/en/master/sections/Releases.html#case-studies>

with  $TECH$  and  $RES$  the sets of all the technologies and resources, respectively, and  $\text{lifetime}(j)$  the lifetime of the technology  $j$ .  $\mathbf{E}_{\text{constr}}(j)$  and  $\mathbf{E}_{\text{op}}(i)$  are the system annual energy invested in construction of technology  $j$  and operation of resource  $i$ , respectively. They are defined as follows

$$\mathbf{E}_{\text{constr}}(j) = e_{\text{constr}}(j)\mathbf{F}(j) \quad \forall j \in TECH, \quad (3a)$$

$$\mathbf{E}_{\text{op}}(i) = \sum_{t \in \mathcal{T} \setminus \{h, td\} \in T\_H\_TD(t)} e_{\text{op}}(i)\mathbf{F}_t(i, h, td)t_{\text{op}}(h, td) \quad \forall i \in RES, \quad (3b)$$

with  $e_{\text{constr}}(j)$  [GWh/GW] the specific value of energy invested in construction of technology  $j$  which is the cumulative energy demand associated to the construction of this technology,  $e_{\text{op}}(i)$  [GWh/GWh<sub>fuel</sub>] the specific value of energy invested in operation of resource  $i$  which includes extraction/production/transportation and combustion,  $\mathbf{F}(j)$  [GW] ([GWh] for storage technologies) the installed capacity of the technology  $j$ ,  $\mathbf{F}_t(i, h, td)$  [GWh] the quantity of the resource  $i$  that is used at the hour  $h$  of the typical day  $td$ ,  $t_{\text{op}}(h, td)$  (1h by default) the time period duration,  $\mathcal{T}$  the set of all the periods of the year, *i.e.*, 8760 hours, and  $T\_H\_TD(t)$  the hour  $h$  and the typical day  $td$  associated to the period  $t$ . In (3b) summing over the different typical days and the hours of typical days, using the set  $T\_H\_TD(t)$ , is equivalent to summing over the 8760 hours of the year.

The choice made in EnergyScope TD to model Climate change is the global warming potential (GWP) [MtCO<sub>2</sub>-eq./y]. The annual greenhouse gas emissions of the system  $\mathbf{GWP}_{\text{tot}}$  are defined as the sum of: (1) the emissions related to the construction and end-of-life of the energy conversion technologies  $\mathbf{GWP}_{\text{constr}}$ , allocated to one year based on the technology lifetime; (2) the emissions related to the operation of resources  $\mathbf{GWP}_{\text{op}}$  which accounts for extraction, transportation and combustion. They are defined as follows

$$\mathbf{GWP}_{\text{tot}} = \sum_{j \in TECH} \frac{\mathbf{GWP}_{\text{constr}}(j)}{\text{lifetime}(j)} + \sum_{i \in RES} \mathbf{GWP}_{\text{op}}(i), \quad (4a)$$

$$\mathbf{GWP}_{\text{constr}}(j) = gwp_{\text{constr}}(j)\mathbf{F}(j) \quad \forall j \in TECH, \quad (4b)$$

$$\mathbf{GWP}_{\text{op}}(i) = \sum_{t \in \mathcal{T} \setminus \{h, td\} \in T\_H\_TD(t)} gwp_{\text{op}}(i)\mathbf{F}_t(i, h, td)t_{\text{op}}(h, td) \quad \forall i \in RES. \quad (4c)$$

Similarly to the energy invested, the total emissions related to the construction of technologies are the product of the specific emissions  $gwp_{\text{constr}}$  and the installed capacity  $\mathbf{F}$ . The total emissions of resources operation are the emissions associated with fuels from cradle to combustion and imports of electricity  $gwp_{\text{op}}$  multiplied by

the quantities of resources used  $\mathbf{F}_t(i, h, td)$  and the period duration  $t_{\text{op}}$ .

The GHG emissions scenario or target is defined by setting a limit,  $gwp_{\text{limit}}$ , on the annual system GHG emissions  $\mathbf{GWP}_{\text{tot}}$  as follows

$$\mathbf{GWP}_{\text{tot}} \leq gwp_{\text{limit}}. \quad (5)$$

Therefore, the method relies on a snapshot approach [35] where for two different GHG emissions targets specified in (5) two different strategies result from the optimization without a pathway to link them with each other.

In practice,  $\text{EROI}_{\text{fin}}$  (1) is computed ex-post by using the optimization result with

$$E_{\text{out}} = \text{FEC}, \quad (6a)$$

$$E_{\text{in}} = \arg \min \mathbf{E}_{\text{in,tot}}, \quad (6b)$$

where the final energy consumption (FEC) is derived from the simulation result with the methodology detailed in [Appendix B](#).

GWP data ( $gwp_{\text{op}}$  and  $gwp_{\text{constr}}$ ) are estimated by using a life cycle assessment (LCA) approach taken from the Ecoinvent database v3.2 [41] using the “allocation at the point of substitution”, *i.e.*, taking into account emissions of technologies and resources “from the cradle to the grave” and following the indicator “GWP100a-IPCC2013” developed by the Intergovernmental Panel on Climate Change (IPCC) [42]. The “Input Data” Section of the online documentation provides the input data to apply the EnergyScope TD model to the Belgian energy system in 2035. Table 2 summarizes the specific value of energy invested  $e_{\text{op}}(i)$  and  $gwp_{\text{op}}(i)$  and GHG emissions for each resource in 2035. We refer the reader to the online documentation for the data related to the construction of technologies.

Finally, EnergyScope TD has an hourly resolution and a tractable formulation with a few minutes of computational time computationally affordable due to twelve typical days [2]. This number allows to reach a good trade-off with: (i) a limited impact on the resulting energy system strategy, *i.e.*, the installed capacity of the technologies and the use of resources remain in the same order of magnitude; (ii) a significant gain in computational time from 20 hours, with no typical day, to a few minutes. This relatively short computation time allows: (1) for a detailed analysis of the high integration of renewable energy resources and storage capacities; (2) to keep the uncertainty quantification, several thousands of runs.

Resources	$gwp_{op}$	$e_{op}$
Elec. import	206	0.123
NG	267	0.0608
Renewable gas	0	0.269
Gasoline	345	0.281
Bio-ethanol	0	0.316
Diesel	315	0.21
Bio-diesel	0	0.432
LFO	312	0.204
H2	364	0.083
Renewable H2	0	0.579
Ammonia	285	0.065
Renewable ammonia	0	0.579
Methanol	350	0.0798
Renewable methanol	0	0.579
Wood	11.8	0.0491
Wet biomass	11.8	0.0559
Waste	150	0.0577
Uranium	3.9	0.0434
Wind	0	0
Solar	0	0
Hydro	0	0
Geothermal	0	0

Table 2: The specific value of energy invested  $e_{op}$  [GWh/GWh<sub>fuel</sub>] and GHG emissions  $gwp_{op}$  [MtCO<sub>2</sub>-eq./y] for each resource in 2035 used in the case study. The GHG emissions are given for the impact of the resources combustion only, based on Quaschning [43]. And the methodology of the data collection of  $e_{op}$  relies on Muyldermans and Nève [22] where the data have been collected from the *ecoinvent* database [41].

### 3. Case study: the 2035 Belgian energy system

The model is applied to the 2035 Belgian energy system for several GHG emission targets. This year is a trade-off between a long-term horizon where policies can still be implemented and a horizon short enough to define the future of the society with a group of known technologies.

#### 3.1. Case study description

The energy transition relies on renewable energies, making their deployment potential a critical parameter. Tables 3 and 4 provide the installed capacity of technologies using renewable energy and the renewable resource potential, respectively. The data for 2015 and

	Technology	2015	2020	2035
Electricity production	PV	3.85	4.49	59.2 <sup>†</sup>
	onshore wind	1.49	2.49	10
	offshore wind	0.70	1.95	6
	hydro river	0.11	0.115	0.115
Heat production	geothermal	0	0	0
	geothermal	0	0	0
	cen. solar th.	0	0	70 <sup>†</sup>
	dec. solar th.	0	0	70 <sup>†</sup>

Table 3: Comparison of installed capacity [GWe] or [GWth] of technologies using renewable energy in 2015, 2020 and their maximal potential expected in the model for 2035. <sup>†</sup> PV and solar thermal technologies compete with the land availability constraint of 250km<sup>2</sup> which is equivalent to 59.2 GWe of PV or 70 GWth of solar thermal (centralized or decentralized). 2015 and 2020 data are based on European Commission et al. [24] and the 2035 projection on Limpens et al. [23]. Abbreviations: centralized (cen.), decentralized (dec.), thermal (th.).

2020 are compared to the predictions for 2035 used as input parameters of the model. In the following paragraphs, we comment on some of the parameters considered in the case study.

Based on the current policies, Belgium intends to phase out coal and nuclear. Hence, we suppose coal and nuclear power plants are shut down in 2035; thus not available. However, in the sensitivity analysis conducted in Section 5, the installed nuclear capacity is considered an uncertain parameter. A limit of 27.9% [23] of the 2035 electricity end-use demand, representing 27.57 [TWh/y], bounds the electricity imports and restricts the Belgian electrical dependence on neighboring countries. This study assumes an upper limit of 59.2 GWe [23] of PV installed capacity. This estimation relies on two hypotheses; (i) the actual area of available well-oriented roofs is approximatively 250km<sup>2</sup> [44], which is around 1% of total Belgian lands; (ii) a 23% PV efficiency expected in 2035 with an average daily total irradiation, similar to historical values, of 2820 Wh/m<sup>2</sup>. Notice that PV and solar thermal technologies compete with this land availability constraint of 250km<sup>2</sup>, equivalent to 59.2 GWe of PV or 70 GWth of solar thermal (centralized or decentralized). This study accounts for two types of biofuels: bio-diesel and bio-ethanol. They can substitute diesel and gasoline, respectively. Finally, a new type of renewable fuel, produced from renewable electricity, is considered. This study allocates them a zero-global warming potential, *i.e.*,  $gwp_{op} = 0$  [MtCO<sub>2</sub>-eq./GWh]. However, there is al-

	Resources	2015	2020	2035
Imported fuels	bio-ethanol	0.48	? <sup>†</sup>	no limit
	bio-diesel	2.89	? <sup>†</sup>	no limit
	gas-RE	0	0	no limit
	H2-RE	0	0	no limit
	ammonia-RE	0	0	no limit
Biomass	methanol-RE	0	0	no limit
	woody	13.9	? <sup>†</sup>	23.4
Waste	wet	11.6	? <sup>†</sup>	38.9
		7.87	? <sup>†</sup>	17.8
Elec. import		24.54	-0.6	27.57

Table 4: Comparison of renewable resources [TWh] in 2015, 2020, and their maximal potential in the model for the year 2035. Waste is a non-renewable resource. <sup>†</sup> no consolidated data available. Abbreviations: electricity (elec.), renewable (RE).

ways a residual CO<sub>2</sub>-impact that must be compensated for through biomass or direct air capture. Nevertheless, the analysis of these CO<sub>2</sub>-compensation approaches is out of the scope of this work. Four fuels are considered: hydrogen, ammonia, methanol, and methane. They can be “renewable” or fossil with a  $gwp_{op} > 0$  [MtCO<sub>2</sub>-eq./GWh].

The 2035 heating, electricity, and mobility EUD projections are based on Limpens et al. [23] and Table 5 summarizes the differences between the EUD in 2015, 2020 and 2035. It is possible to notice the COVID-19 impact in 2020. The 2035 passenger transport demand, 194 [Mpass.-km/y], is divided between public and private transport. The lower and upper bounds for the use of public transport are 19.9% and 50% of the annual passenger transport demand, respectively. The freight demand, 98 [Mt-km/y], can be supplied by trucks, trains, or inland boats with corresponding lower and upper bounds: 0% and 100%, 10.9% and 25% 15.6% and 30%, respectively.

### 3.2. Reference case study results

EnergyScope TD reaches an EROI-optimum Belgian energy system in 2035 at around 8.9 and 100.3 [MtCO<sub>2</sub>-eq./y] without limiting the GHG emissions. This case is called “reference scenario-100%”, where the constraint (5) is not activated, and the parameters are at nominal values. In comparison, the EU reference scenario 2020 [24] provides the actual 2015 and 2020 values and the 2035 forecast value for the total GHG emissions<sup>6</sup>

<sup>6</sup>These GHG emissions values do not consider the international intra-EU and international extra-EU and Use, Land-Use Change and

EUD	2015	2020	2035
Electricity [TWhe]	81.5	74.8	91.9
Heat high T. [TWh]	74.1	71.2	50.4
Heat low T. [TWh]	124.8	116.8	147.3
Non-energy [TWh]	89.0	86.3	53.1
Mobility pass. [Mpass.-km]	147	110	194
Mobility freight [Mt-km]	70	69	98

Table 5: Comparison of EUD for 2015, 2020, and the 2035 projection. The 2015 and 2020 heat low/high T. EUD are derived from the FEC of the corresponding sector (residential, service and industry for heat low T. and energy intensive industries for heat high T.) by removing the corresponding electricity FEC. 83.1% of the electricity FEC of Belgium is allocated to the residential, service and industry sectors and the remaining to the energy intensive industries sector. This ratio is estimated based on European Commission and Eurostat [45]. 2015 and 2020 data are based on European Commission et al. [24] and the 2035 projection on Limpens et al. [23]. Abbreviations: end-use demand (EUD), temperature (T.), passenger (pass.), tons (t).

of 118.6, 106.6, and 100.0 [MtCO<sub>2</sub>-eq./y], respectively. Notice that 2020 is particular due to the COVID-19, and the GHG emissions are expected to increase in the coming years before decreasing to achieve the EU targets. As explained in the following paragraphs, the 2035 energy system, when maximizing the EROI, relies mainly on natural gas, which is less carbon-intensive than the actual Belgian energy system, which uses oil for mobility. In addition, the share of renewable energies is higher with maximal wind installed capacities.

Non-renewable sources (82.7%), particularly natural gas (NG) import, dominate the primary energy mix (413 TWh): NG import (292.9 TWh), methanol (38.4 TWh), ammonia (10.2 TWh). Renewables stand only for 17.1% of the primary energy supply and are split between wind (43.0 TWh), wood (23.4 TWh), solar (4.0 TWh), and hydro (0.5 TWh). The remaining 0.2% consists of electricity import (0.8 TWh). Table 6 details the major technologies used to supply the demands of Table 5 in terms of share of production and installed capacity. The electricity generation relies mainly on gas with CCGT (33.4 TWh) and CHP (65.8 TWh) vs. wind (43.0 TWh), PV (4.0 TWh), hydro (0.5 TWh), and imported electricity (0.8 TWh). A large part of the electricity production (42.3 TWh) is used to supply heat pumps which supply mainly DEC and DHN low-temperature heat demands. The gas CHP is the most prominent player in supplying the industrial high-temperature heat demand, besides a small share from gas boilers. Overall, mobility is also dominated by NG import: (1) passenger

Forestry (LULUCF).

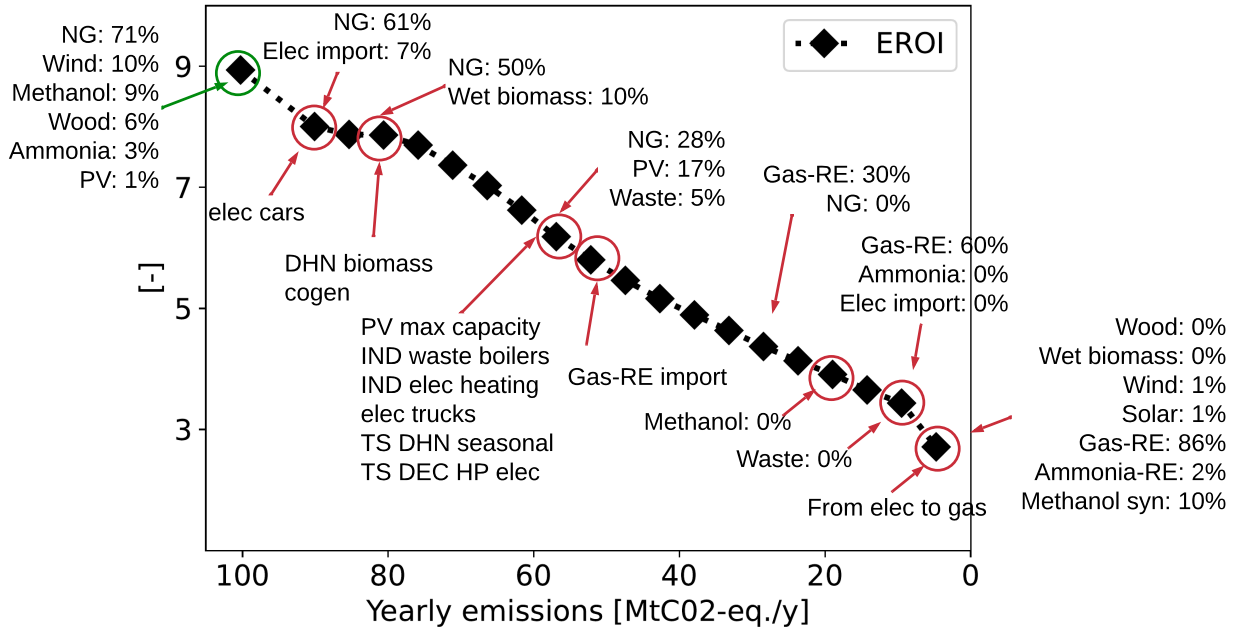


Figure 3: EROI - GHG emissions optima with primary energy mix and technologies implementation. The energy transition is composed of seven main steps illustrated with the red circles. Abbreviations: natural gas (NG), electricity (elec), district heating networks (DHN), decentralized (DEC), heat pump (HP), thermal storage (TS), industrial (IND), maximal (max), renewable gas (Gas-RE).

mobility is equally divided between private (50%) and public (50%) technologies with NG cars (100% of the private mobility), tramways (30% of the public mobility), trains (50% of the public mobility), and NG buses (20% of the public mobility); (3) NG trucks, trains, and NG boats for the road, train, and boat freight, respectively. Finally, methanol and ammonia are imported to satisfy the non-energy demand, where a large part of the methanol is used to synthesize high-value chemicals (HVC).

The result of an EROI-optimum for the 2035 Belgian energy system of 8.9 is close to the estimation of the 2018 societal worldwide EROI [12]. However, this comparison suffers from two limitations. First, in their model, the current global energy system was mainly based on fossil fuels in 2018. Second, the scope of their study differs as it considers the world. EnergyScope TD with the reference scenario indicates that renewable synthetic fuels are too energy-expensive to compete against the fossil equivalent when there is no constraint on GHG emissions. However, it is essential to remind that such a system results from linear optimization. A slight difference, *e.g.*, efficiency, energy invested in construction or operation, can make the system switch between two different solutions but with similar energy invested objective. This is another rationale to account for

uncertainties in such a research field, which is investigated in Section 5.

#### 4. Results: EROI Belgian energy transition

This Section conducts an analysis of the Belgian energy system in 2035 by forcing the total annual emissions of the system to decrease by reducing its upper limit, *i.e.*,  $gwp_{\text{limit}}$  in (5). In practice, 5% steps of  $GWP_{\text{tot}}$  reduction were made from the  $GWP_{\text{op}}$  (94.9 [MtCO<sub>2</sub>-eq./y]) of the “reference scenario-100%” presented in Section 3.2. First, we investigate energy trends system strategies by considering the EROI in the objective function facing different GHG emissions constraints. However, it is essential to note that these strategies result from specific snapshot optimizations without a pathway to link them with each other. Then, we compare a solution maximizing the system EROI to a solution minimizing the system cost.

##### 4.1. EROI of the system evolution

The GHG emissions target scenarios are analyzed from two perspectives: (1) the evolution of the EROI and GHG of the system; (2) the primary energy supply and its use in the energy system. Appendix C provides

Demand	Technology	Production	Capacity
Electricity	CCGT	33.4	6.5
	wind	43.0	16.0
	PV	4.0	3.9
Heat HT	gas CHP	59.7	8.0
	gas boiler	4.2	4.8
Heat LT DHN	HP	45.2	12.9
	gas CHP	7.0	4.3
Heat LT DEC	HP	92.9	31.3
Private mobility	gas car	97.0	-
Public mobility	train	48.5	-
	tramway	29.1	-
	gas bus	19.4	-
Freight	gas truck	44.1	-
	gas boat	29.4	-
	train	24.5	-

Table 6: Reference scenario-100%: major technologies used to supply the demands of Table 5 in terms of production and installed capacity. The private mobility accounts for 50% of the passengers mobility. Units: production of electricity and all types of heat in [TWh], the private and public mobility in [Mpass.-km], the freight mobility in [Mt-km], and the production capacity of electricity and all types of heat in [GW]. Abbreviations: end-use demand (EUD), high temperature (HT), low temperature (LT), combined cycle gas turbine (CCGT), combined heat and power (CHP), decentralized (DEC), district heating networks (DHN), passenger (pass.), heat pump (HP), natural gas (NG).

additional results presented in terms of installed capacities, energy invested, and final energy consumption for the different GHG emissions targets.

#### 4.1.1. System evolution summary

Figure 3 depicts a summary of the EROI - GHG emissions optima with primary energy mix and technologies implementation. The system shifts from high emissions to low emissions; however, this is a view of the mind because the solutions of each GHG emissions target scenario do not represent a transition path and must be analyzed individually. In the following, we comment on the energy transition in seven steps, the red circles depicted in Figure 3.

Step 0 - “reference scenario-100%” - green circle depicted in Figure 3:  $GWP_{tot}$  reaches 100.3 [MtCO<sub>2</sub>-eq./y], and the system energy primary mix relies on 71% of NG and the related technologies to satisfy the electricity, heat, and mobility demand (see Section 3.2).

Step 1 -  $gwp_{limit} = 90.1$  [MtCO<sub>2</sub>-eq./y]: the system is

partially electrified with a shift from NG to electric cars for private mobility. In addition, a part of the electricity production shifts from CCGT to electricity import, reaching 7% of the primary energy mix. The NG share in the primary energy mix dropped by 10% and reached 61%.

Step 2 -  $gwp_{limit} = 80.6$  [MtCO<sub>2</sub>-eq./y]: wet biomass is introduced and achieves 10% of the primary energy mix. DHN biomass co-generation technology supplies the DHN heat low-temperature demand instead of DHN gas co-generation. There is an additional decrease of 10% of the NG share in the primary energy mix.

Step 3 -  $gwp_{limit} = 61.7$  [MtCO<sub>2</sub>-eq./y]: PV technology and waste resource achieve the maximal available capacity with 59.2 [GWe] and 17.8 [GWh], representing 17% and 5% of the primary energy mix, respectively. Waste boilers and direct electricity heating replace the industrial gas boilers. The trucks shift from NG to electricity. Thermal seasonal and daily storage are introduced to cope with the solar and wind seasonal and daily intermittency.

Step 4 -  $gwp_{limit} = 56.9$  [MtCO<sub>2</sub>-eq./y]: synthetic renewable gas (gas-RE) begins to be imported. Then, when  $gwp_{limit} = 33.2$  [MtCO<sub>2</sub>-eq./y], the NG disappears from the primary energy mix, and the gas-RE import amounts to 30% of the primary energy mix.

Step 5 -  $gwp_{limit} = 19.0$  [MtCO<sub>2</sub>-eq./y]: the imported methanol and the waste resource ( $gwp_{limit} = 14.2$  [MtCO<sub>2</sub>-eq./y]) disappear from the primary energy mix.

Step 6 -  $gwp_{limit} = 9.5$  [MtCO<sub>2</sub>-eq./y]: the imported ammonia and electricity vanish from the primary energy mix. The gas-RE import amounts to 60% of the primary energy mix. CCGT technology replaces the electricity imports to produce electricity by using the gas-RE.

Step 7 -  $gwp_{limit} = 4.7$  [MtCO<sub>2</sub>-eq./y]: there is an extreme shift from electric-based to gas-based technologies. Indeed, the wood, wet biomass, wind, and solar energies have almost completely vanished from the primary energy mix. The gas-RE, ammonia-RE, and methanol-RE imports amount to 86%, 2%, and 10% of the primary energy mix, respectively. The cars and trucks shift from electric to gas technologies using the gas-RE. The CCGT produces electricity with gas-RE. Finally, boilers and co-generation using gas-RE satisfy the heat demand.

The following paragraphs comment in detail on the breakdown of GHG emissions by resources and technologies, and the evolution of the system primary energy mix.

#### 4.1.2. System GHG emissions

Figure 4 depicts the system  $\mathbf{GWP}_{\text{constr}}$  and  $\mathbf{GWP}_{\text{op}}$  breakdown by technologies and resources for the different yearly GHG emissions targets in 2035. The GHG construction emissions are mainly driven by electricity and mobility technologies. The PV installation amounts to a significant part of the electricity construction GHG emissions increase between GHG emissions targets of 80.6 and 61.7 [MtCO<sub>2</sub>-eq./y]. Private passenger mobility composes the prominent part of the mobility construction GHG emissions with battery-electric cars for GHG emissions targets between 90.1 and 9.5 [MtCO<sub>2</sub>-eq./y], and NG cars for the reference case and the GHG emissions target of 4.7 [MtCO<sub>2</sub>-eq./y]. The GHG operation emissions mainly comprise non-renewable resources: NG, electricity import, methanol, and ammonia. They decrease with the progressive shift from non-renewable to renewable resources.

#### 4.1.3. System primary energy evolution

Figure 5 depicts the system primary energy evolution for several yearly GHG emissions targets in 2035 breakdown by resource categories. Step 0 - “reference scenario-100%”: the primary energy mix comprises mainly NG with a share of 71%. Renewable resources are composed of wind, solar, and wood. Onshore and offshore wind resources are used at the maximum available capacity with 10 [GWe] and 6 [GWe]. They amount to 10.4% of the primary energy mix. The wood represents 5.7% of the primary energy and is also used at its maximum capacity of 23.4 [GWh/y]. Finally, the PV capacity is 3.9 [GWe] and amounts to only 1% of the primary energy mix. Indeed, the energy invested in constructing offshore and onshore wind capacities is approximately two times lower than the PV capacity.

Figure 6 provides the system primary energy evolution breakdown between non-renewable and renewable resources, respectively. The following comments explain the main steps of non-renewable resources decrease. Step 1 -  $\mathbf{gwp}_{\text{limit}} = 90.1$  [MtCO<sub>2</sub>-eq./y]: the decrease of NG in the primary energy mix is balanced with electricity import<sup>7</sup>, which reaches the maximum importation limit of 27.5 [GWh/y]. The other non-renewable and renewable resources are stable in volume compared to the “reference scenario-100%”. Step 2 -  $\mathbf{gwp}_{\text{limit}} = 80.6$  [MtCO<sub>2</sub>-eq./y]: wet biomass and solar renewable resources balance the NG decrease. The wet biomass is

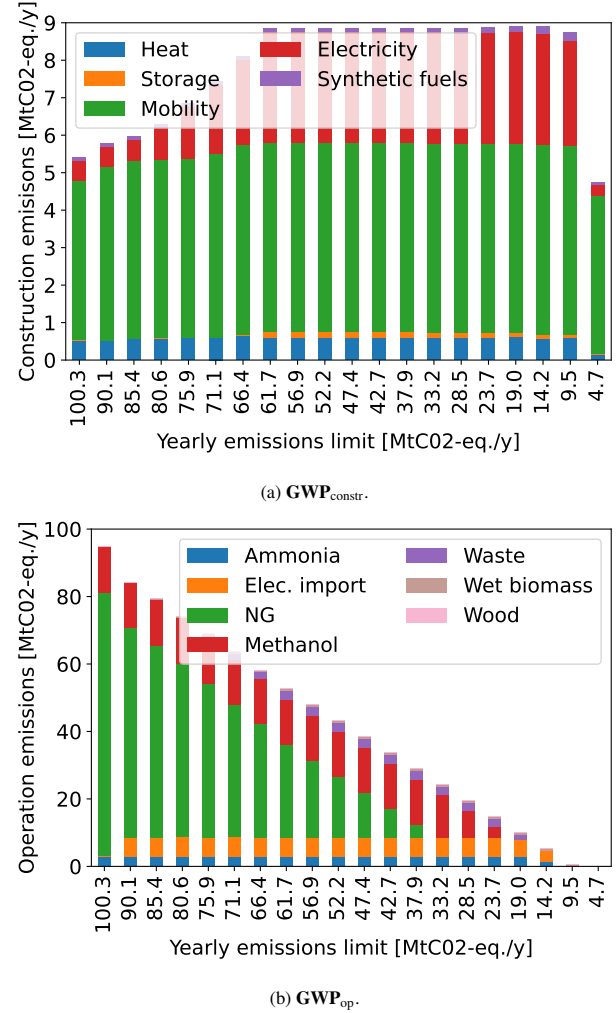


Figure 4: System  $\mathbf{GWP}_{\text{constr}}$  and  $\mathbf{GWP}_{\text{op}}$  breakdown by technologies and resources for several yearly GHG emissions targets in 2035.

used at its maximal capacity of 38.9 [GWh/y]. The PV capacity starts to increase and reaches a capacity of 11.2 [GWe]. Then, from 80.6 to 61.7 [MtCO<sub>2</sub>-eq./y], the NG decrease is balanced with increased waste and PV in the primary energy mix. The latter reaches the maximal installed capacity of 59.2 [GWe]. Step 3 -  $\mathbf{gwp}_{\text{limit}} = 61.7$  [MtCO<sub>2</sub>-eq./y]: NG amounts to 28.1%, PV 16.8%, wind offshore and onshore 11.7%, wood 6.4%, biomass 10.6%, and waste 4.9% of the primary energy mix. Steps 4 to 6 - from 61.7 to 9.5 [MtCO<sub>2</sub>-eq./y]: the decrease in NG, methanol, waste, and electricity imports is progressively balanced by importing renewable gas (gas-RE). Step 7 -  $\mathbf{gwp}_{\text{limit}} = 4.7$  [MtCO<sub>2</sub>-eq./y]: below 9.5 [MtCO<sub>2</sub>-eq./y], there are no more non-renewable resources. GHG emissions targets force the system to decrease the construction GHG emissions as the op-

<sup>7</sup>The use of imported electricity is highly dependent on its indirect emissions. In this study, electricity imports emit about half of the electricity production of a CCGT. Therefore, imported electricity replaces the production of CCGTs.

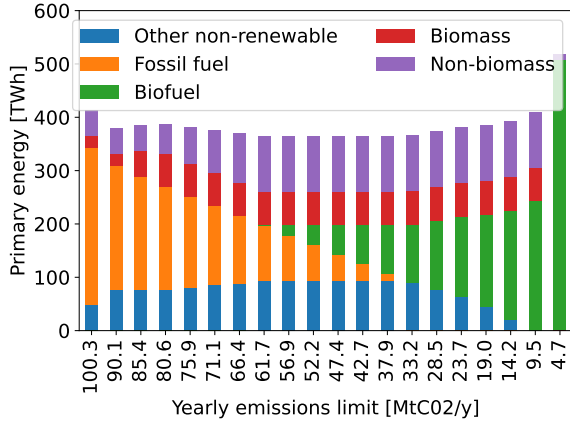


Figure 5: System primary energy mix evolution for several yearly GHG emissions targets in 2035 breakdown by resource categories. Abbreviations: non-RE: waste, methanol, and ammonia; Fossil: NG; RE-fuels: gas-RE, methanol-RE, and ammonia-RE; Biomass: wood, and wet biomass.

eration GHG emissions are approximately 0 [MtCO<sub>2</sub>-eq./y]. Renewable fuels almost completely replace the PV and wind resources, and the system is partially un-electrified to use them. For instance, electric vehicles (mobility private and freight) are replaced by vehicles using synthetic fuels. That case is hypothetical because it assumes that: (1) imported renewable fuels imply lower GHG emissions than renewable resources such as solar and wind. However, the GWP data on renewable fuels are not mature enough to draw such conclusions; (2) it is doubtful to import such quantities of renewable fuels (approximately 510 [TWh/y]).

#### 4.1.4. Conclusion

The system EROI evolution analysis provides two main conclusions. First, major energy system changes occur when the system  $\mathbf{GWP}_{\text{tot}} \leq 9.5$  [MtCO<sub>2</sub>-eq./y]. In this case, the domestic renewable energies such as solar and wind are replaced by imported renewable fuels and electric technologies by gas-based technologies. Almost all the primary energy is composed of renewable fuels. This case is not realistic and depends on the quality of GWP and energy invested data which are uncertain for renewable fuels. In addition, it is unexpected to import approximately 510 [TWh/y] of such renewable fuels. Thus, further investigations need to be conducted to investigate low carbon energy system with  $\mathbf{GWP}_{\text{tot}} \leq 10$  [MtCO<sub>2</sub>-eq./y]. Second, renewable fuels seem to play an increasingly key role in the energy transition to satisfy the mobility and heating end-use demands when decreasing GHG emissions. They repre-

sent the major part of the system primary energy when  $\mathbf{GWP}_{\text{tot}} \approx 10$  [MtCO<sub>2</sub>-eq./y]. These preliminary results encourage further investigations to assess the impact of the data quality, particularly synthetic fuels, on the results. Thus, Section 5 conducts a sensitivity analysis of the system EROI for several GHG emissions targets above 10 [MtCO<sub>2</sub>-eq./y].

#### 4.2. Comparative study: system EROI when minimizing the cost vs. the invested energy

Figure 7 depicts the evolution of the cost and EROI of the 2035 system for several GHG emissions scenarios when minimizing the cost and maximizing the EROI. The trends are similar. The EROI of the system decreases when constraining the GHG emissions, and the EROI level is constantly smaller for a given GHG emissions target when minimizing the system cost. Similarly, the cost of the system is constantly higher for a given GHG emissions target when minimizing the energy invested in the system.

However, the primary energy mix differs, as illustrated by Figure 8. When minimizing the system cost, with no GHG emissions target, the system uses a higher share of domestic renewable resources with 41.9 [TWh/y] of onshore and offshore wind, 33.8 [TWh/y] of PV, 23.4 [TWh/y] of wood, and 38.9 [TWh/y] of wet biomass. In comparison, when maximizing the system EROI, the system uses 43 [TWh/y] of wind onshore and offshore, 4 [TWh/y] of PV, 23.4 [TWh/y] of wood, and 0 [TWh/y] of wet biomass. In addition, the system uses a smaller share of NG, which is compensated with more renewable energies, coal, light oil fuel (LFO), waste, and electricity import. When the GHG emissions decrease, the fossil energies are progressively replaced by imported renewable fuels: ammonia, methanol, H<sub>2</sub>, and renewable gas. Indeed, domestic renewable energies are almost already used at maximal capacity, except for the PV with 32.2 [GWe] when there is no restriction on GHG emissions.

Overall, the strategy to decrease GHG emissions is similar when minimizing the system cost and maximizing the EROI by importing an increased share of renewable fuels. However, instead of using large quantities of imported renewable gas, the system also employs renewable ammonia, methanol, and H<sub>2</sub>. The renewable ammonia is employed in CCGT to produce electricity, and the renewable gas in CHP is consumed to satisfy a part of the high-temperature heat demand. The methanol is converted into HVC, and the H<sub>2</sub> is used for the freight. Finally, the wet biomass produces renewable gas with the bio-methanation process instead of being directly consumed in CHP, and boilers consume

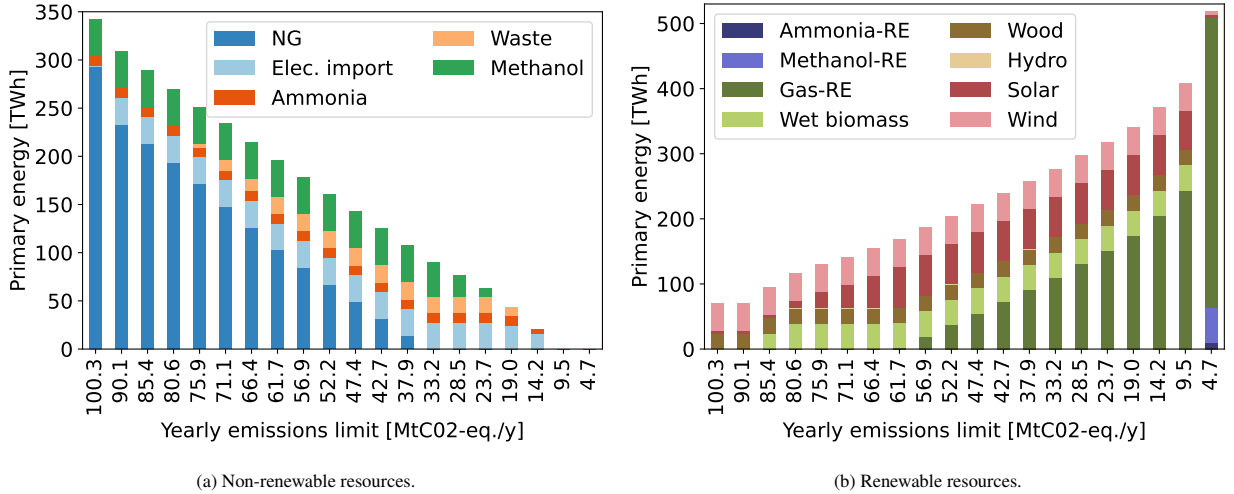


Figure 6: System primary energy mix evolution for several yearly GHG emissions targets in 2035 breakdown between non-renewable and renewable resources. Abbreviations: NG: natural gas, Elec. import: electricity import; renewable fuels: gas-RE, methanol-RE, and ammonia-RE; hydro: hydro river.

the wood to satisfy the heat high-temperature demand instead of being transformed into methanol.

## 5. Sensitivity analysis of the system EROI

The model relies on numerical input data, which are sometimes highly uncertain, such as the energy invested in the operation of renewable fuels. This uncertainty could influence the key messages of the previous deterministic results. To nuance these messages, two actions are proposed: (i) being transparent on the dataset used (refer to the online documentation), (ii) assessing the impact of uncertainty of the system EROI for several GHG emissions targets through global sensitivity analysis (GSA), and the Monte Carlo method. This section is an extension of the works of Limpens [46], Rixhon et al. [21] by assessing the uncertainty of the EROI of the system with a GSA using the polynomial chaos expansion (PCE) method [47]. The PCE approach emphasizes the critical parameters by using Sobol indices and extracting statistical moments, mean and variance, of the EROI of the system.

This section is organized into two parts. First, the most critical uncertain parameters for the EROI of the system are listed according to their respective Sobol indices based on the GSA results. Then, the EROI of the system is analyzed through its mean, variance, and probability density function (pdf). Appendix D provides the details about the GSA approach and additional results concerning the first and second-order PCE.

### 5.1. Critical parameters

The PCE coefficients allow estimating the statistical moments, *e.g.*, mean  $\mu$  and variance  $\sigma$ , of the EROI of the system, without additional computational cost. In addition, it enables the estimation of the EROI pdf by a Monte Carlo approach with the obtained surrogate model in a few seconds of computational time.

Figure 9 illustrates the evolution of the Top-5 parameters and their total-order Sobol values [%] for GHG emissions of 28.5 and 85.4 [MtCO<sub>2</sub>-eq./y] over several GHG emissions targets. The total-order Sobol value of a parameter indicates its contribution to the variance of the EROI of the system. Table 7 presents the Top-5 critical parameters for several GHG emissions targets with the values of the total-order Sobol indices.

It is expected that  $e_{\text{op}}^{\text{Gas-RE}}$  becomes the primary driver of the variation of the EROI of the system, given the increasing share of renewable gas in the primary energy mix when GHG emissions targets decrease. In the model, the energy invested in the operation of renewable gas is 4.4 higher than its fossil equivalent, making it less competitive; thus, unused with no restrictions on GHG emissions. However, it becomes the most-impacting parameter, up to 67.1% of the variance of the EROI of the system for the GHG emissions target of 19.0 [MtCO<sub>2</sub>-eq./y]. The lower part of Figure 9 illustrates the opposite trend for NG. Given its low energy invested in operation, it is a critical resource when the GHG emissions targets are not compelling. The energy invested in the construction of gas cars and NG operation substantially impacts the EROI variance with 39.2% and 25.5%, re-

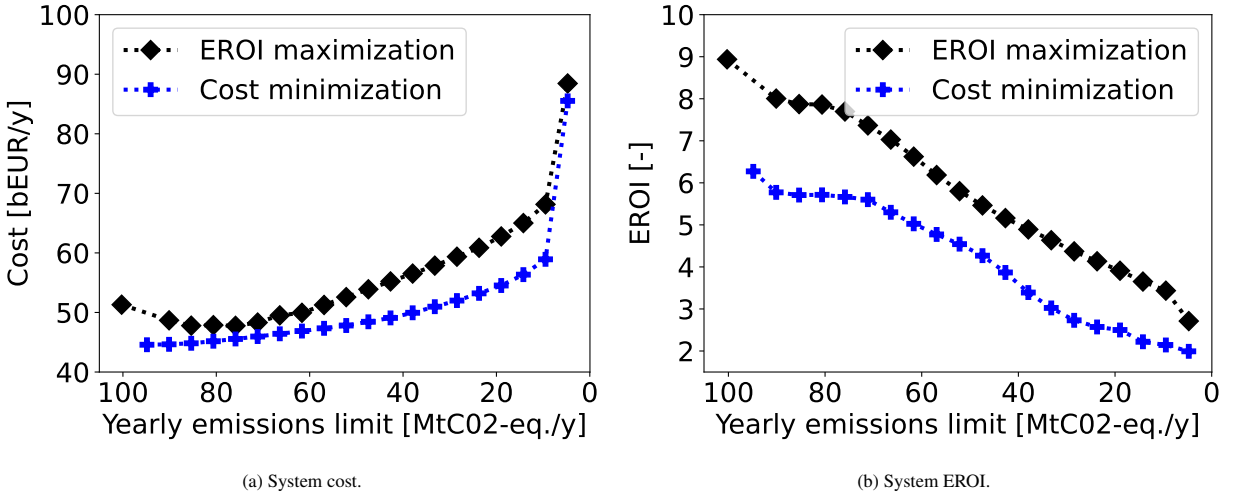


Figure 7: Comparison of the system cost and EROI evolution for several scenarios of GHG emissions when minimizing the cost and maximizing the EROI.

Ranking	85.4	56.9	28.5	19.0
1	$e_{\text{constr}}^{\text{NG cars}}$ 39.2	$e_{\text{constr}}^{\text{Elec. cars}}$ 18.0	$e_{\text{op}}^{\text{Gas-RE}}$ 43.6	$e_{\text{op}}^{\text{Gas-RE}}$ 67.1
2	$e_{\text{op}}^{\text{NG}}$ 25.5	$f_{\text{max}}^{\text{NUC}}$ 12.5	$e_{\text{constr}}^{\text{Elec. cars}}$ 4.8	$e_{\text{constr}}^{\text{Elec. cars}}$ 6.1
3	$e_{\text{constr}}^{\text{Elec. cars}}$ 6.3	$\%_{\text{public mob}}^{\text{max}}$ 7.7	$f_{\text{max}}^{\text{NUC}}$ 4.8	$f_{\text{max}}^{\text{NUC}}$ 3.4
4	$\%_{\text{public mob}}^{\text{max}}$ 5.4	$e_{\text{constr}}^{\text{PV}}$ 5.0	$\text{avail}^{\text{Wet biomass}}$ 4.7	$\text{avail}^{\text{Wood}}$ 2.5
5	$e_{\text{op}}^{\text{Wet biomass}}$ 4.3	$e_{\text{op}}^{\text{NG}}$ 5.0	$f_{\text{max}}^{\text{Offshore wind}}$ 4.2	$\%_{\text{public mob}}^{\text{max}}$ 2.3

Table 7: Top-5 critical parameters and their total-order Sobol values [%] for several GHG emissions targets [MtCO<sub>2</sub>-eq./y]. Abbreviations: electric (elec.) photovoltaic (PV), nuclear (NUC), renewable gas (Gas-RE), natural gas (NG). Table D.11 in Appendix D.4 lists all the critical parameters with their total-order Sobol values [%].

spectively, when the GHG emissions are weakly constrained (85.4 [MtCO<sub>2</sub>-eq./y]).

Then, the energy invested in the construction of electric cars  $e_{\text{constr}}^{\text{Elec. cars}}$  is the second parameter to play a key role in the variance of the EROI of the system with the decrease of GHG emissions. It is the most-impacting parameter on the system EROI with 18.0%, for the target of 56.9 [MtCO<sub>2</sub>-eq./y]. Then, it is the second most-impacting parameter with 4.8% and 6.1%, for the targets of 28.5 and 19.0 [MtCO<sub>2</sub>-eq./y]. Figure C.16 depicts the essential impact on the system EROI of the private mobility for GHG emissions between 61.7 and 9.5 [MtCO<sub>2</sub>-eq./y], where the energy invested in construction is mainly composed of mobility and electricity technologies, and more particularly of PV and electric cars.

The maximum capacity of nuclear power plants  $f_{\text{max}}^{\text{NUC}}$  is the third critical parameter. It has lower energy invested in construction than PV, 2600 vs. 4400 [GWh/GW], which is similar to wind on/offshore, and a

negligible related global warming potential of construction. Thus, the system consistently relies on the maximum capacity of the nuclear power plant.  $f_{\text{max}}^{\text{NUC}}$  is the second most-impacting parameter with 12.5% for GHG emissions target of 56.9 [MtCO<sub>2</sub>-eq./y], and the third one with 4.8% and 3.4% for targets of 28.5 and 19.0 [MtCO<sub>2</sub>-eq./y].

The wet biomass  $\text{avail}^{\text{Wet biomass}}$  and wood  $\text{avail}^{\text{Wood}}$  availabilities with 4.7% and 2.5%, respectively, are the fourth critical parameters for low GHG emissions targets of 28.5 and 19.0 [MtCO<sub>2</sub>-eq./y]. The energy invested in the operation of the wood is lower than biomass, 0.049 vs. 0.056 [GWh/GWh] for an equivalent global warming potential. The wood is used by the model to produce methanol for satisfying the non-energy demand. Thus, it allows limiting the methanol importations, which have a higher invested in the operation with 0.08 [GWh/GWh].

Finally, for GHG emissions targets of 28.5 and 19.0 [MtCO<sub>2</sub>-eq./y], [MtCO<sub>2</sub>-eq./y], the fifth critical param-

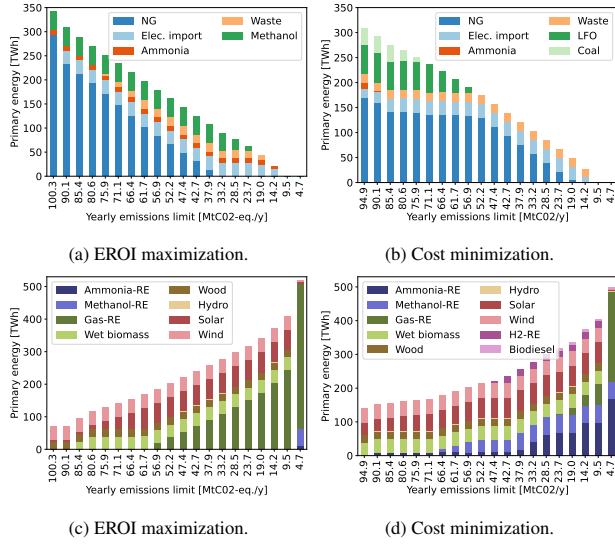


Figure 8: Comparison of the system primary energy mix breakdown by non-renewable resources (upper) and renewable resources (lower) for several scenarios of GHG emissions when minimizing the cost (left) and maximizing the EROI (right).

eters are the offshore wind maximal installed capacity  $f_{max}^{Offshore\ wind}$  and the maximal share of public mobility  $\%_{max}^{public\ mob}$  with 4.2% and 2.3%, respectively. Private car is the most significant partaker in the passenger mobility of Belgium. According to the Federal Planning Bureau [48], 80% of the passenger mobility is expected to be supplied by private cars in the future. Therefore, it supports half of the passenger mobility, and the other half is supplied by public transport modes, *i.e.*, buses, trains, and tramways. Thus, the uncertainty on the maximal share of public mobility  $\%_{max}^{public\ mob}$  is likely to impact significantly private mobility and the system EROI.

### 5.2. EROI probability density functions

Figure 10 depicts the EROI mean  $\mu$  and the evolution of the 95% ( $\pm 2\sigma$  in gray) confidence interval for the GHG emissions targets considered. Table 8 presents the mean, the standard deviation of the system EROI, and the coefficient of variation (CoV), defined as the ratio between  $\sigma$  and  $\mu$ . Finally, Figure 11 presents the EROI pdf for each GHG emissions target using the Monte Carlo approach along with the mean depicted by the dashed vertical line.

Phasing out of low energy-intensive fossil fuels, particularly NG, by relying on more renewables and importing renewable fuels naturally drives down the system EROI. This EROI decrease raises concerns about a minimal system EROI value below which a prosperous lifestyle would not be sustainable. The estimation of

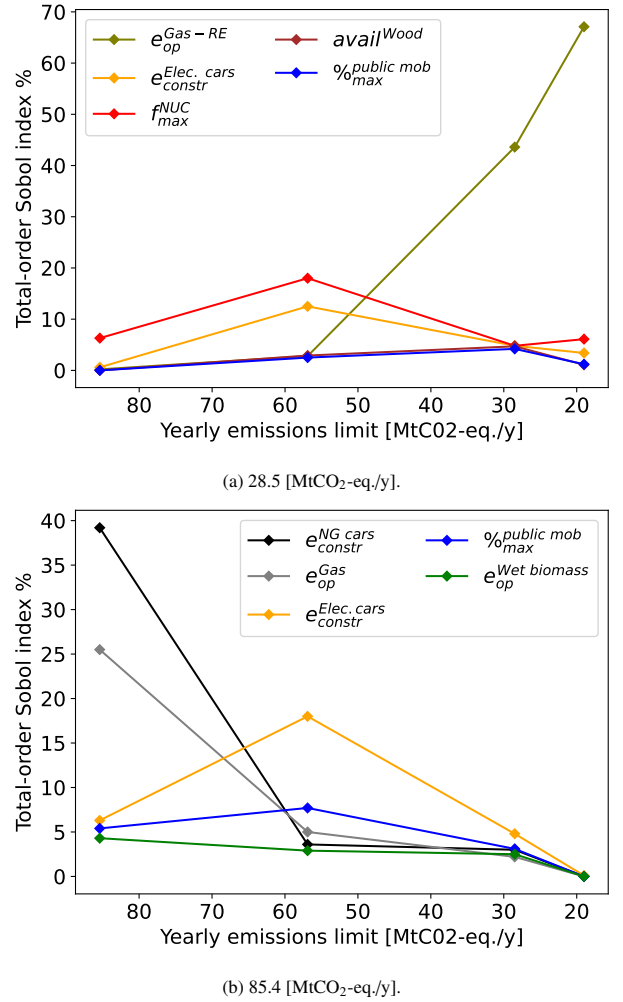


Figure 9: Evolution of the total-order Sobol values of the Top-5 critical parameters for GHG emissions of 28.5 and 85.4 [MtCO<sub>2</sub>-eq./y].

such value is complex and out of the scope of this study. However, it is possible that considering the actual values of energy invested in the construction of renewable technologies and the operation of renewable resources, the system EROI could reach this limit before achieving carbon neutrality. The estimated system EROI probability density functions indicate that decreasing the GHG emissions makes the EROI more sensitive to uncertain parameters. Indeed, the 95% confidence interval ( $\pm 2\sigma$ ) narrows slower than the decrease in the mean. This trend is translated in an increase in the CoV with 9.0 % *vs.* 10.5% for GHG emissions targets of 85.4 and 19.0 [MtCO<sub>2</sub>-eq./y], as depicted in Table 8. These results reinforce the importance of considering the uncertainties of parameters in long-term energy planning. In addition, in this case, deterministic optimization underesti-

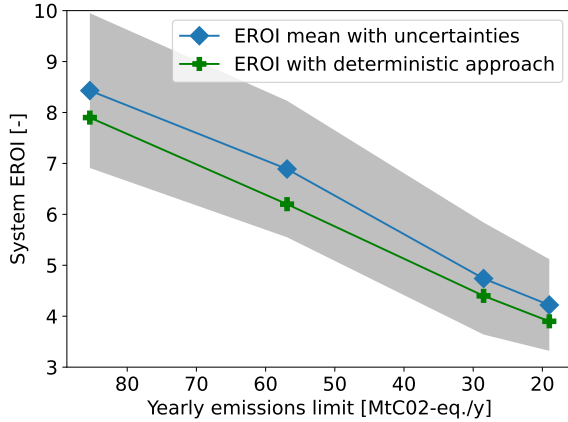


Figure 10: The EROI mean  $\mu$  (blue curve) of the runs performed during the sensitivity analysis with the 95% confidence interval ( $\pm 2\sigma$  in gray), and the result of the deterministic runs at the nominal value of the parameters (green curve).

GWP <sub>tot</sub> [MtCO <sub>2</sub> -eq./y]	85.4	56.9	28.5	19.0
Deterministic	7.9	6.2	4.4	3.9
Mean $\mu$	8.4	6.9	4.7	4.2
Standard deviation $\sigma$	0.76	0.67	0.55	0.45
CoV $\sigma/\mu$ [%]	9.0	9.7	11.6	10.5

Table 8: Deterministic value, mean, standard deviation of the system EROI, and ratio between  $\sigma$  and  $\mu$ , the coefficient of variation (CoV).

mates the system EROI on average of 6-7% and cannot provide a confidence interval. The maximal nuclear capacity  $f_{max}^{NUC}$  is responsible for this underestimation, set to 0 [GWe] in the deterministic setting. This parameter is considered uncertain in stochastic settings with a uniform distribution between 0 and 5.6 [GWe]. Then, the model systematically uses the nuclear capacity at its maximal value; thus, increasing the EROI as the energy invested in constructing nuclear power plants is similar to wind on/offshore.

## 6. Discussion and limitations

This section first discusses the results of Sections 4 and 5. Then, it presents the limitations of the model and the methodology used to perform the sensitivity analysis of the system EROI.

### 6.1. Discussion

Overall, this study provides the following primary outcomes when maximizing the system EROI: (1) renewable energies (domestic such as solar and wind or

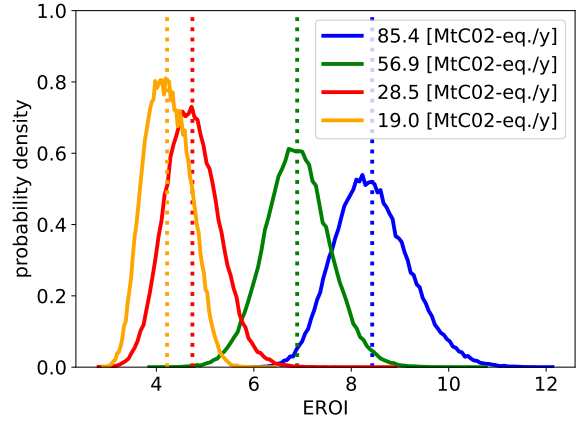


Figure 11: Probability density function (plain lines) of the system EROI for several GHG emissions targets. The dashed vertical lines provide the EROI mean of the runs performed during the sensitivity analysis: 8.4, 6.9, 4.7, and 4.2 for 85.4, 56.9, 28.5, and 19.0 [MtCO<sub>2</sub>-eq./y], respectively.

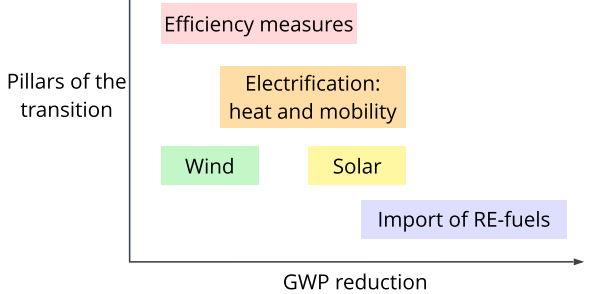


Figure 12: The pillars of the energy transition to decrease the GHG emissions when maximizing the system EROI.

imported with renewable fuels) are required massively to reach ambitious GHG emissions targets; (2) nuclear energy is not the primary driver of the EROI variance.

Concerning the first point, given its limited domestic renewable potential compared to its end-use demands, Belgium has to import energy-intensive renewable fuels to decrease GHG emissions. The uncertainty of the energy invested in the operation of these renewable fuels drives up the variance of the system EROI. This result is similar to the simulations with the minimization of the system cost [21, 23], where the uncertainties of the renewable fuels prices are responsible for the increase of the system cost variance. Figure 12 depicts the key pillars of the energy transition when decreasing the GHG emissions. The system sequentially uses most of the options of the energy Mix scenario [23], which is a scenario accounting for an increased amount of renewable resources plus nuclear capacity and geother-

mal energy, but with a different priority. The model begins with low-energy intensive fossil (NG) and domestic renewable resources (wind) when there is no limit on GHG emissions. Then, it first improves its energy efficiency in the early stages by reducing the primary energy consumed to meet the demand. The electrification is progressively performed with the electricity imports at their full potential (27.57 [TWh/y]) to improve the electrification of the mobility (private electric vehicles) and heating sectors (heat pumps). Then, to enhance the electrification while reducing the overall global warming potential, the system uses local PV renewable electricity production up to its full potential of 59.2 [GWe], and wet biomass 38.9 [TWh/y] and waste 17.8 [TWh/y] for heating. Finally, the model forces the system to import renewable fuels massively to achieve ambitious low GHG emissions targets. When maximizing the EROI, the system uses mainly renewable gas, and when minimizing the cost, it is a mix of H<sub>2</sub>, renewable gas, and renewable-liquid fuels (ammonia and methanol). These pillars indicate the main levers to decrease GHG emissions while maximizing the system EROI and the research directions to decrease the uncertainties of the parameters of the related technologies and resources. Indeed, efforts should not be distributed equally to decrease the uncertainties of every model parameter. The sensitivity analysis provides the critical uncertain parameters responsible for the main contributions to the system EROI variance. A similar conclusion to Rixhon et al. [21], Limpens et al. [23] is drawn: policymakers, industries, and academia should spend time and energy improving the knowledge about renewable fuels by reducing the cost, the energy invested in the operation, and the related uncertainties.

Concerning the second point, the sensitivity analysis reveals the impact of the maximum capacity of the nuclear power plant on the variance of the system EROI. The contribution of this parameter reaches a maximum of 12.5% for the GHG emissions target of 56.9 [MtCO<sub>2</sub>-eq./y]. Then, it decreases to 3.4% at 19.0 [MtCO<sub>2</sub>-eq./y] and is never the main driver of the EROI variation for all GHG emissions targets considered. Therefore, nuclear electricity does not compete against renewables, either local or imported. In addition, it substantially improves the system EROI as the model always utilizes nuclear power plants at their maximal capacity.

## 6.2. Limitations

The study limitations are either caused by the model or the uncertainty characterization and quantification conducted in the EROI sensitivity analysis.

First, we depict three main model limitations: (1) the snapshot approach [35] limits the concept of a trajectory between several GHG emissions targets. One way to overcome this issue is to consider a pathway [46, Chapter 7] that could describe the different steps continuously in terms of technologies to implement and resources to exploit; (2) the unlimited availability of imported renewable fuels regardless of origin. Estimating the realistic maximal import quantities of imported renewable fuels could be done with different costs and energy invested in operation concerning the origin. For instance, the study Colla et al. [49] proposes a framework to account for the different origin of biomass imports; (3) the linear optimization approach makes the results highly sensitive to the input parameters. A slight difference in technology efficiency or energy invested in construction or operation can make the system switch between two different solutions but with a similar objective. The sensitivity analysis partially addresses this issue because it relies on the relevant definition of the list of uncertain parameters with their uncertainty range. Another approach could consist of investigating the feasible space near optimality. The study Dubois and Ernst [50] proposes a generic framework for addressing this issue. It allows looking for solutions that can accommodate different requirements, such as determining necessary conditions on the minimal energy investments in domestic renewable energies or imported renewable fuels.

Finally, we propose four main limitations concerning the uncertainty characterization and quantification: (1) the energy data invested in the construction of technology and the operation of resources. The methodology of the data collection relies on Muyldermans and Nève [22] where the data have been obtained from the *ecoinvent* database Wernet et al. [41]. However, new data and publications could refine these values, especially for renewable fuels, which are booming; (2) the global warming potential data in the operation of renewable resources, particularly renewable fuels, is assumed to be 0. New data and publications could refine these values, similar to the energy data invested data; (3) the choice of uncertain parameters. This study focuses mainly on energy invested related parameters and did not consider other parameters such as the technology efficiencies and lifetimes or the GWP of construction and operation. A complete investigation should be conducted to consolidate the results; (4) the uncertainty ranges considered are based on Moret et al. [51], Rixhon et al. [21] for the parameters not related to the energy invested in construction and operation. However, these ranges could be updated based on the last data and publications re-

leases. In addition, due to the significant uncertainty of the energy invested in the construction and operation of technologies and resources, we adopted an arbitrary uncertainty range of minus/plus 25%. Further work should be dedicated to refining this range and adapting it to specific technology and resource.

## 7. Conclusion

Most long-term policies to decrease the carbon footprint of our societies consider the cost of the system as the leading indicator in the energy system models. However, the energy transition encompasses economic, technical, environmental, and social aspects. We consider a more comprehensive indicator to address this issue: the EROI of a whole-energy system.

The primary outcomes of this paper are: (1) assessing the EROI of a whole energy system by extending the EnergyScope TD [2] model and providing open access to the Python code and the database; (2) the investigation of the transition of the 2035 Belgian energy system by considering the EROI of the system; (3) the comparison of the results of the system cost minimization to the system EROI maximization; (4) the global sensitivity analysis of the EROI of the system by applying a polynomial chaos expansion method [47]. It provides the critical drivers of the variation of the system EROI; (5) the estimation of the probability density functions of the EROI of the system for several GHG emissions targets.

The main results are fivefold. First, the EROI of the system decreases from 8.9 to 3.9 for GHG emissions of 100 and 19 [MtCO<sub>2</sub>-eq./y]. These values can be put into perspective with estimated values of: (i) lower bound on the societal EROI, *e.g.*, 5 [9, 11] or 6 [10]; (ii) worldwide EROI, *e.g.*, 8.5 [12] in 2018 and 12 [17] in 2015. Second, the renewable fuels - mainly imported renewable gas - represent the largest share of the system primary energy mix when GHG emissions decrease due to the lack of endogenous renewable resources such as wind and solar. Third, the strategy to decrease GHG emissions is similar when minimizing the cost of the system and maximizing the EROI. It consists of importing an increased share of renewable fuels to reduce GHG emissions. However, instead of using large quantities of imported renewable gas, the system also employs renewable ammonia, methanol, and H<sub>2</sub>. The EROI of the system, when minimizing the cost, decreases from 6.3 to 2.5 for GHG emissions of 95 and 19 [MtCO<sub>2</sub>-eq./y]. Fourth, the sensitivity analysis reveals that the energy invested in the operation of renewable

gas is responsible for 67.1% of the variation of the system EROI for the GHG emissions target of 19 [MtCO<sub>2</sub>-eq./y]. Finally, the estimation of the EROI probability density functions exhibits that decreasing the GHG emissions makes the EROI of the system more variable to uncertain parameters. Indeed, the coefficient of variation, which is the ratio of the standard deviation over the mean, increases with GHG emissions reduction.

The decrease of the EROI of the system with the GHG emissions raises questions on meeting the climate targets without adverse socio-economic impact. Thus, we hope these results will encourage policymakers, industries, and academia to: (i) dedicate more research to assess whole-energy systems with the EROI indicator; (ii) spend more time and energy improving the knowledge about renewable fuels, mainly to decrease the uncertainties related to their cost, availability, and energy invested.

Future works will address the model limitations, *e.g.*, drawing a continuous plan of strategies from today to the carbon neutrality of 2050 instead of the snapshots approach. They will also focus on refining the data and reducing the uncertainties of the main drivers, *i.e.*, the renewable fuels, of the variation of the system EROI. In addition, the EnergyScope TD model could be extended to: (i) assess the EROI of a system composed of several inter-connected countries by using EnergyScope Multi-Cell [38], such as Europe to better take into account the domestic complementarity of renewables; (ii) perform multi-criteria optimization in the vein of Muylleldmans and Nève [22] with indicators such as the system cost, global warming potential, and EROI; (iii) include a macroeconomic model following the approach of Dupont et al. [12] to estimate another indicator, introduced by Fagnart and Germain [52], called the net energy ratio (NER) of the economy. The NER is more comprehensive than the EROI and allows assessing the energy embodied in the intermediate and capital consumptions of the entire economy.

## 8. Acknowledgments

The authors would like to acknowledge the authors and contributors of the EnergyScope TD model and RHEIA<sup>8</sup> [53] Python library. In addition, we acknowledge professor Hervé Jeanmart, President of the Institute of Mechanics, Materials, and Civil engineering (IMMC) and at the Catholic University of Louvain. He

---

<sup>8</sup><https://rheia.readthedocs.io/en/latest/>

has facilitated the collaboration of the teams and provided helpful insights and discussions about the present work.

## References

- [1] V. Masson-Delmotte, P. Zhai, A. Pirani, S. Connors, C. Péan, S. Berger, N. Caud, Y. Chen, L. Goldfarb, M. Gomis, M. Huang, K. Leitzell, E. Lonnoy, J. Matthews, T. Maycock, T. Waterfield, O. Yelekçi, R. Yu, Z. B. IPCC, 2021: Summary for Policymakers. In: Climate Change 2021: The Physical Science Basis. Contribution of Working Group I to the Sixth Assessment Report of the Intergovernmental Panel on Climate Change, Technical Report, Intergovernmental Panel on Climate Change, 2021. URL: <https://www.ipcc.ch/assessment-report/ar6/>.
- [2] G. Limpens, S. Moret, H. Jeanmart, F. Maréchal, Energyscope td: A novel open-source model for regional energy systems, *Applied Energy* 255 (2019) 113729. URL: <https://www.sciencedirect.com/science/article/pii/S0306261919314163>. doi:<https://doi.org/10.1016/j.apenergy.2019.113729>.
- [3] C. J. Cleveland, R. Costanza, C. A. S. Hall, R. Kaufmann, Energy and the u.s. economy: A biophysical perspective, *Science* 225 (1984) 890–897. URL: <https://www.science.org/doi/abs/10.1126/science.225.4665.890>. doi:[10.1126/science.225.4665.890](https://doi.org/10.1126/science.225.4665.890).
- [4] C. Hall, M. Lavine, J. Sloane, Efficiency of energy delivery systems: I. an economic and energy analysis, *Environmental Management* 3 (1979) 493–504. doi:<https://doi.org/10.1007/BF01866318>.
- [5] K. Mulder, N. J. Hagens, Energy return on investment: toward a consistent framework, *AMBITO: A Journal of the Human Environment* 37 (2008) 74–79. doi:[https://doi.org/10.1579/0044-7447\(2008\)37\[74:EROITA\]2.0.CO;2](https://doi.org/10.1579/0044-7447(2008)37[74:EROITA]2.0.CO;2).
- [6] J. G. Lambert, C. A. Hall, S. Balogh, A. Gupta, M. Arnold, Energy, eroi and quality of life, *Energy Policy* 64 (2014) 153–167. URL: <https://www.sciencedirect.com/science/article/pii/S0301421513006447>. doi:<https://doi.org/10.1016/j.enpol.2013.07.001>.
- [7] C. A. Hall, J. G. Lambert, S. B. Balogh, Eroi of different fuels and the implications for society, *Energy Policy* 64 (2014) 141–152. URL: <https://www.sciencedirect.com/science/article/pii/S0301421513003856>. doi:<https://doi.org/10.1016/j.enpol.2013.05.049>.
- [8] P. E. Brockway, A. Owen, L. I. Brand-Correa, L. Hardt, Estimation of global final-stage energy-return-on-investment for fossil fuels with comparison to renewable energy sources, *Nature Energy* 4 (2019) 612–621.
- [9] C. A. S. Hall, S. Balogh, D. J. Murphy, What is the minimum eroi that a sustainable society must have?, *Energies* 2 (2009) 25–47. URL: <https://www.mdpi.com/1996-1073/2/1/25>. doi:[10.3390/en20100025](https://doi.org/10.3390/en20100025).
- [10] V. Court, An estimation of different minimum exergy return ratios required for society, *BioPhysical Economics and Resource Quality* 4 (2019) 1–13. URL: <https://link.springer.com/article/10.1007/s41247-019-0059-6>. doi:<https://doi.org/10.1007/s41247-019-0059-6>.
- [11] A. R. Brandt, How does energy resource depletion affect prosperity? mathematics of a minimum energy return on investment (eroi), *BioPhysical Economics and Resource Quality* 2 (2017) 1–12. URL: <https://link.springer.com/article/10.1007/s41247-017-0019-y>. doi:<https://doi.org/10.1007/s41247-017-0019-y>.
- [12] E. Dupont, M. Germain, H. Jeanmart, Estimate of the societal energy return on investment (eroi), *Biophysical Economics and Sustainability* 6 (2021) 1–14. doi:<https://doi.org/10.1007/s41247-021-00084-9>.
- [13] J. Lambert, C. Hall, S. Balogh, Eroi of global energy resources: Status, trends and social implications, 2013. doi:[10.13140/2.1.2419.8724](https://doi.org/10.13140/2.1.2419.8724).
- [14] M. R. Sers, P. A. Victor, The energy-emissions trap, *Ecological Economics* 151 (2018) 10–21. URL: <https://www.sciencedirect.com/science/article/pii/S0921800917317044>. doi:<https://doi.org/10.1016/j.ecolecon.2018.04.004>.
- [15] F. Contino, S. Moret, G. Limpens, H. Jeanmart, Whole-energy system models: The advisors for the energy transition, *Progress in Energy and Combustion Science* 81 (2020) 100872. URL: <https://www.sciencedirect.com/science/article/pii/S0360128520300824>. doi:<https://doi.org/10.1016/j.pecs.2020.100872>.
- [16] M. Borasio, S. Moret, Deep decarbonisation of regional energy systems: A novel modelling approach and its application to the italian energy transition, *Renewable and Sustainable Energy Reviews* 153 (2022) 111730. URL: <https://www.sciencedirect.com/science/article/pii/S1364032121010030>. doi:<https://doi.org/10.1016/j.rser.2021.111730>.
- [17] I. Capellán-Pérez, C. De Castro, L. J. M. González, Dynamic energy return on energy investment (eroi) and material requirements in scenarios of global transition to renewable energies, *Energy Strategy Reviews* 26 (2019) 100399. URL: <https://www.sciencedirect.com/science/article/pii/S2211467X19300926>. doi:<https://doi.org/10.1016/j.esr.2019.100399>.
- [18] I. Capellán-Pérez, I. de Blas, J. Nieto, C. de Castro, L. J. Miguel, O. Carpintero, M. Mediavilla, L. F. Lobejón, N. Ferreras-Alonso, P. Rodrigo, et al., Medeas: a new modeling framework integrating global biophysical and socioeconomic constraints, *Energy Environ. Sci.* 13 (2020) 986–1017. URL: <http://dx.doi.org/10.1039/C9EE02627D>. doi:[10.1039/C9EE02627D](https://doi.org/10.1039/C9EE02627D).
- [19] X. Rixhon, M. Colla, D. Tonelli, K. Verleysen, G. Limpens, H. Jeanmart, F. Contino, Comprehensive integration of the non-energy demand within a whole-energy system: Towards a defossilisation of the chemical industry in belgium, 2021. URL: [https://best-energy.be/wp-content/uploads/2021/08/Xavier\\_ECOS2021-Presentation-Condensed.pdf](https://best-energy.be/wp-content/uploads/2021/08/Xavier_ECOS2021-Presentation-Condensed.pdf), under sounmission for publication.
- [20] G. Limpens, H. Jeanmart, Electricity storage needs for the energy transition: An eroi based analysis illustrated by the case of belgium, *Energy* 152 (2018) 960–973. URL: <https://www.sciencedirect.com/science/article/pii/S0360544218305899>. doi:<https://doi.org/10.1016/j.energy.2018.03.180>.
- [21] X. Rixhon, G. Limpens, D. Coppitters, H. Jeanmart, F. Contino, The role of electrofuels under uncertainties for the belgian energy transition, *Energies* 14 (2021). URL: <https://www.mdpi.com/1996-1073/14/13/4027>. doi:[10.3390/en14134027](https://doi.org/10.3390/en14134027).
- [22] B. Muylldermans, G. Nève, Multi-criteria optimisation of an energy system and application to the Belgian case, Master's thesis, UCL - Ecole polytechnique de Louvain, 2021. URL: <http://hdl.handle.net/2078.1/thesis:33139>.
- [23] G. Limpens, H. Jeanmart, F. Maréchal, Belgian energy transition: What are the options?, *Energies* 13 (2020). URL: <https://www.mdpi.com/1996-1073/13/1/261>. doi:[10.3390/en13010261](https://doi.org/10.3390/en13010261).

[24] European Commission, Directorate-General for Climate Action, Directorate-General for Energy, Directorate-General for Mobility and Transport, A. De Vita, P. Capros, L. Paroussos, K. Fragkiadakis, P. Karkatsoulis, L. Höglund-Isaksson, W. Winiwarter, P. Purohit, A. Gómez-Sanabria, P. Rafaj, L. Warnecke, A. Deppermann, M. Gusti, S. Frank, P. Lauri, F. Fulvio, A. Florou, M. Kannavou, N. Forsell, T. Fotiou, P. Siskos, P. Havlík, I. Tsipopoulos, S. Evangelopoulou, P. Witzke, M. Kesting, N. Katoufa, I. Mitsios, G. Asimakopoulou, T. Kalokyris, EU reference scenario 2020 : energy, transport and GHG emissions : trends to 2050, Publications Office, 2021. URL: [https://energy.ec.europa.eu/data-and-analysis/energy-modelling/eu-reference-scenario-2020\\_en](https://energy.ec.europa.eu/data-and-analysis/energy-modelling/eu-reference-scenario-2020_en). doi:[10.2833/35750](https://doi.org/10.2833/35750).

[25] D. Devogelaer, D. Gusbin, Bon vent: setting sail for a climate neutral belgian energy system, 2021. URL: [https://www.plan.be/publications/publication-2172-en-bon\\_vent\\_setting\\_sail\\_for\\_a\\_climate\\_neutral\\_belgian\\_energy\\_system\\_future\\_belgian\\_offshore\\_wind\\_unravelled](https://www.plan.be/publications/publication-2172-en-bon_vent_setting_sail_for_a_climate_neutral_belgian_energy_system_future_belgian_offshore_wind_unravelled), [accessed 28-March-2022].

[26] F. Meinke-Hubeny, L. P. de Oliveira, J. Duerinck, P. Lodewijks, R. Belmans, Energy transition in belgium-choices and costs, 2017. URL: <https://www.energyville.be/energy-transition-belgium-choices-and-costs>.

[27] Elia, Electricity scenarios for belgium towards 2050, 2017. URL: <https://www.elia.be/en/publications/studies-and-reports>, [accessed 28-March-2022].

[28] RTE, Energy pathways to 2050: Key results, 2021. URL: <https://www.rte-france.com/analyses-tendances-et-prospectives/bilan-prévisionnel-2050-futurs-énergétiques#Lesdocuments>, [accessed 31-March-2022].

[29] European Commission, Modelling tools for eu analysis, 2022. URL: [https://ec.europa.eu/clima/eu-action/climate-strategies-targets/economic-analysis/modelling-tools-eu-analysis\\_en](https://ec.europa.eu/clima/eu-action/climate-strategies-targets/economic-analysis/modelling-tools-eu-analysis_en).

[30] Artelys, Artelys crystal super grid, 2022. URL: <https://www.artelys.com/crystal/super-grid/>, [accessed 19-April-2022].

[31] L. G. Fishbone, H. Abilock, Markal, a linear-programming model for energy systems analysis: Technical description of the bnl version, International journal of Energy research 5 (1981) 353–375. doi:<https://doi.org/10.1002/er.4440050406>.

[32] M. Doquet, R. Gonzalez, S. Lépy, E. Momot, F. Verrier, A new tool for adequacy reporting of electric systems: Antares, CIGRE 2008 session, paper C1-305, Paris (2008).

[33] RTE, Antares-simulator, 2022. URL: <https://antares-simulator.org/>, [accessed 19-April-2022].

[34] S. Moret, Strategic energy planning under uncertainty, Ph.D. thesis, EPFL-École Polytechnique Fédérale de Lausanne, 2017. URL: <http://infoscience.epfl.ch/record/231814>. doi:[10.5075/epfl-thesis-7961](https://doi.org/10.5075/epfl-thesis-7961).

[35] V. Codina Gironès, S. Moret, F. Maréchal, D. Favrat, Strategic energy planning for large-scale energy systems: A modelling framework to aid decision-making, Energy 90 (2015) 173–186. URL: <https://www.sciencedirect.com/science/article/pii/S0360544215007136>. doi:<https://doi.org/10.1016/j.energy.2015.06.008>.

[36] R. Martinez, J. Maria, Study of the Spanish Energy Transition, Master's thesis, UCL - Ecole polytechnique de Louvain, 2021. URL: <http://hdl.handle.net/2117/353583>.

[37] J. Dommisse, J.-L. Typhon, Modelling of low carbon energy systems for 26 european countries with EnergyScopeTD : can european energy systems reach carbon neutrality independently ?, Master's thesis, UCL - Ecole polytechnique de Louvain, 2020. URL: <http://hdl.handle.net/2078.1/thesis:25202>.

[38] P. Thiran, A. Hernandez, H. Jeanmart, G. Limpens, EnergyScope Multi-Cell: a novel open-source model for multi-regional energy systems and application to a 3-cell, low-carbon energy system, Master's thesis, UCL - Ecole polytechnique de Louvain, 2020. URL: <http://hdl.handle.net/2078.1/thesis:25229>.

[39] N. Cornet, P. Eloy, H. Jeanmart, G. Limpens, Energy exchanges between countries for a future low-carbon Western Europe: merging cells in EnergyScope MC to handle wider regions, Master's thesis, UCL - Ecole polytechnique de Louvain, 2021. URL: <http://hdl.handle.net/2078.1/thesis:33090>.

[40] P. Thiran, A. Hernandez, G. Limpens, M. G. Prina, H. Jeanmart, F. Contino, Flexibility options in a multi-regional whole-energy system: the role of energy carriers in the italian energy transition, in: The 34th International Conference on Efficiency, Cost, Optimization, Simulation and Environmental Impact of Energy Systems, 2021, pp. 407–416. URL: <https://www.proceedings.com/062738-0037.html>. doi:<https://doi.org/10.52202/062738-0037>.

[41] G. Wernet, C. Bauer, B. Steubing, J. Reinhard, E. Moreno-Ruiz, B. Weidema, The ecoinvent database version 3 (part i): overview and methodology, The International Journal of Life Cycle Assessment 21 (2016) 1218–1230. doi:<https://doi.org/10.1007/s11367-016-1087-8>.

[42] T. Stocker, D. Qin, G.-K. Plattner, M. Tignor, S. Allen, J. Boschung, A. Nauels, Y. Xia, V. Bex, P. Midgley, IPCC, 2013: Climate Change 2013: The Physical Science Basis. Contribution of Working Group I to the Fifth Assessment Report of the Intergovernmental Panel on Climate Change, Technical Report, Intergovernmental Panel on Climate Change, 2013. URL: <https://www.ipcc.ch/report/ar5/wg1/>.

[43] V. Quaschning, Regenerative Energiesysteme: Technologie-Berechnung-Simulation, Carl Hanser Verlag GmbH Co KG, 2015.

[44] D. Devogelaer, D. Gusbin, J. Duerinck, W. Nijs, Y. Marenne, M. Orsini, M. Pairon, Towards 100% renewable energy in belgium by 2050, 2012. URL: [https://www.plan.be/publications/publication-1191-fr-towards\\_100\\_renewable\\_energy\\_in\\_belgium\\_by\\_2050](https://www.plan.be/publications/publication-1191-fr-towards_100_renewable_energy_in_belgium_by_2050), [accessed 31-March-2022].

[45] European Commission and Eurostat, Energy balance sheets – 2016 data : 2018 edition, Publications Office, 2018. URL: <https://op.europa.eu/en/publication-detail/-/publication/38fe1b6c-af7d-11e8-99ee-01aa75ed71a1/language-en>. doi:[doi:10.2785/02631](https://doi.org/10.2785/02631).

[46] G. Limpens, Generating energy transition pathways: application to Belgium, Ph.D. thesis, UCL-Université Catholique de Louvain, 2021.

[47] B. Sudret, Polynomial chaos expansions and stochastic finite element methods, CRC Press Boca Raton, FL, USA, 2014, pp. 265–300.

[48] F. P. Bureau, Perspectives de l'évolution de la demande de transport en belgique à l'horizon 2030, 2015. URL: <https://www.plan.be/publications/publication-1515-en>, [accessed 21-March-2022].

[49] M. Colla, J. Blondeau, H. Jeanmart, Optimal use of lignocellulosic biomass for the energy transition, including the non-energy demand: The case of the belgian energy system, Frontiers in Energy Research 10 (2022). URL: <https://www.frontiersin.org/article/10.3389/fenrg.2022.802327>. doi:[10.3389/fenrg.2022.802327](https://doi.org/10.3389/fenrg.2022.802327).

802327.

[50] A. Dubois, D. Ernst, Computing necessary conditions for near-optimality in capacity expansion planning problems, 2021. URL: <https://arxiv.org/abs/2109.14272>, accepted for publication in PSCC 2022.

[51] S. Moret, V. Codina Gironès, M. Bierlaire, F. Maréchal, Characterization of input uncertainties in strategic energy planning models, Applied Energy 202 (2017) 597–617. URL: <https://www.sciencedirect.com/science/article/pii/S0306261917306116>. doi:<https://doi.org/10.1016/j.apenergy.2017.05.106>.

[52] J.-F. Fagnart, M. Germain, Net energy ratio, eroei and the macroeconomy, Structural Change and Economic Dynamics 37 (2016) 121–126. URL: <https://www.sciencedirect.com/science/article/pii/S0954349X16000047>. doi:<https://doi.org/10.1016/j.strueco.2016.01.003>.

[53] D. Coppitters, W. De Paepe, F. Contino, Robust design optimization and stochastic performance analysis of a grid-connected photovoltaic system with battery storage and hydrogen storage, Energy 213 (2020) 118798. URL: <https://www.sciencedirect.com/science/article/pii/S0360544220319058>. doi:<https://doi.org/10.1016/j.energy.2020.118798>.

[54] European Commission, Directorate-General for Climate Action, Directorate-General for Energy, Directorate-General for Mobility and Transport, M. Zampara, M. Obersteiner, S. Evangelopoulou, A. De Vita, W. Winiwarter, H. Witzke, S. Tsani, M. Kesting, L. Paroussos, L. Höglund-Isaksson, D. Papadopoulos, P. Capros, M. Kannavou, P. Siskos, N. Tasios, N. Kouravatakis, P. Karkatsoulis, P. Frangos, A. Gomez-Sanabria, A. Petropoulos, P. Havlik, S. Frank, P. Purohit, K. Fragiadakis, N. Forsell, M. Gusti, C. Nakos, EU reference scenario 2016 : energy, transport and GHG emissions : trends to 2050, Publications Office, 2016. doi:<https://doi.org/10.2833/9127>.

[55] G. Mavromatidis, K. Orehonig, J. Carmeliet, Uncertainty and global sensitivity analysis for the optimal design of distributed energy systems, Applied Energy 214 (2018) 219–238. URL: <https://www.sciencedirect.com/science/article/pii/S0306261918300710>. doi:<https://doi.org/10.1016/j.apenergy.2018.01.062>.

[56] P. Turati, N. Pedroni, E. Zio, Simulation-based exploration of high-dimensional system models for identifying unexpected events, Reliability Engineering & System Safety 165 (2017) 317–330. URL: <https://www.sciencedirect.com/science/article/pii/S0951832016302964>. doi:<https://doi.org/10.1016/j.ress.2017.04.004>.

FC	Fuel cell.
Gas-RE	Synthetic renewable gas.
GEO	Geothermal.
GHG	Greenhouse gas.
GWP	Global warming potential.
H2-RE	Synthetic renewable H2.
HP	Heat pump.
HVC	High value chemicals.
IPCC	Intergovernmental Panel on Climate Change.
LCA	Life cycle assessment.
LFO	Light oil fuel.
LP	Linear programming.
Methanol-RE	Synthetic renewable methanol.
NG	Natural gas.
PCE	Polynomial chaos expansion.
pdf	Probability density function.
PHS	Pumped hydro storage.
RE	Renewable.
RES	Resources.
TECH	Technologies.
PV	Photovoltaic.

#### Variables (**bold**) and parameters

The snapshot approach implicitly considers variables and parameters over a year. For instance,  $E_{in,tot}$  is the annual system energy invested expressed in [GWh/y]. However, for the sake of clarity, we omit the year unit. The variables are in **bold**.

Name	Unit	Description
$E_{in,tot}$	[GWh]	System energy invested.
$E_{constr}(j)$	[GWh]	System energy invested in construction of technology $j$ .
$E_{op}(j)$	[GWh]	System energy invested in operation of resource $i$ .
$F(j)$	[GW or GWh]	Installed capacity of technology $j$ .
$F_t(i, h, td)$	[GWh]	Quantity of resource $i$ used at hour $h$ of typical day $td$ .
$GWP_{tot}$	[MtCO <sub>2</sub> -eq.]	System GHG emissions.
$GWP_{constr}(j)$	[MtCO <sub>2</sub> -eq.]	GHG emissions of construction of technology $j$ .

#### Acronyms

Name	Description
Ammonia-RE	Synthetic renewable ammonia.
CCGT	Combined cycle gas turbine.
CHP	Combined heat and power.
DEC	Decentralized.
DHN	District heating networks.
EROI	Energy return on investment.
ES-TD	EnergyScope Typical Days.
EUD	End-use demand.
FEC	Final energy consumption.

$GWP_{op}(i)$	[MtCO <sub>2</sub> -eq.]	GHG emissions of resource $i$ .
$e_{constr}(j)$	[GWh/GW]	Energy invested in construction of technology $j$ .
$e_{op}(i)$	[GWh/GWh <sub>fuel</sub> ]	Energy invested in operation of resource $i$ .
$gwp_{constr}(j)$	[ktCO <sub>2</sub> -eq.]	GHG emissions for the construction of technology $j$ .
$gwp_{op}(i)$	[ktCO <sub>2</sub> -eq.]	GHG emissions for the operation of resource $i$ .
$gwp_{limit}$ $t_{op}(h, td)$	[MtCO <sub>2</sub> -eq.] [hour]	GHG emissions target. Time period duration of hour $h$ of typical day $td$ .
$lifetime(j)$	[years]	Lifetime of technology $j$ .

Sets and indices	
Name	Description
$j$	Technology index.
$i$	Resource index.
$h$	Hour index.
$td$	Typical day index.
$eud$	End-use demand index.
$T \cdot H \cdot TD(t)$	Hour $h$ and typical day $td$ associated to the time period $t$ .
$TECH$	Set of technologies.
$RES$	Set of resources.
$\mathcal{T}$	Set of all periods of the year.

## Appendix A. Table 1 justifications

The EU reference scenario 2020 [24] uses the Price-Induced Market Equilibrium System (PRIMES) [29] model, which is not in open-access, and the data used as input are not available. It is an update of the previous version published in 2016 [54]. The model is multi-sectors as the “Reference Scenario” projects the impact of macro-economic, fuel price, and technology trends and policies on the evolution of the EU energy system, transport, and GHG emissions. However, this study considers only one scenario, *i.e.*, the “Reference scenario”. In addition, this study does not consider the EROI, and there is no sensitivity analysis.

In the study [25], the Federal Planning Bureau discusses what role offshore wind can play in helping Belgium achieve climate neutrality by the middle of the century. The analysis is multi-sectors by considering the electricity, H<sub>2</sub>, and gas sectors. The model used is Artelys Crystal Super Grid [30], which is not in open-access, and the data used for the study are not available. In particular, this report examines the development of

joint hybrid offshore wind projects that both provide renewable energy capacity and can serve as interconnectors linking different countries. Two different scenarios are defined and studied; thus, this study is considered partially multi-scenarios. However, this study does not consider the EROI, and there is no sensitivity analysis.

The study [26] uses the TIMES/MARKAL model, a reference in scenario analysis. This model is open access [31], but the different versions for each country are not open. This study has adapted the model to the Belgian case and is unavailable. The main assumptions are detailed in the report with some input parameters. However, there is no proper access to all the input data. The TIMES Belgium model includes different technology portfolios for different supply and demand sectors of the energy system and is consequently multi-sectors. The model generates a set of five scenarios where assumptions on three parameters, namely the import capacity for electricity, the fossil fuel prices, and the phase-out of nuclear energy, are being altered. Finally, the scenario analysis with the TIMES Belgium model is based on a system cost optimization approach; thus, it does not consider the EROI.

The study Elia [27] analyzes both short-term and long-term policy options on the future energy mix for Belgium on the path towards 2050. It proposes the “base case scenario”, “decentral scenario”, and “large-scale RES scenario”. On top of these scenarios, different sensitivities are assessed at the 2030 and 2040 time horizons, resulting in additional scenarios. The assumptions of each scenario are detailed, but the input data are not available, and there is no sensitivity analysis. The report focuses on the electricity sector with renewables (PV, onshore and offshore wind, biomass, hydro, and geothermal) and thermal (CCGT, nuclear, and CHP) generation plants, electric demand (heat pumps, electric vehicles), and considers interconnections with neighboring countries. However, it is not multi-sectors as it does not model the non-electric demand of the transportation, heating, and non-energy sectors. The electricity market simulator developed by RTE, Antares [32, 33] is used to perform the electricity market and adequacy simulations. Antares is open-source and calculates the most-economic unit commitment and generation dispatch. Finally, the scenario analysis with the Antares model is based on a system cost optimization approach; thus, it does not consider the EROI.

The objective of the Energy Pathways to 2050 report [28] is to construct and evaluate several possible options for the evolution of the French power system (generation, network, and consumption) to achieve carbon neutrality. To this end, several scenarios are proposed based

on different assumptions, from 100% renewable generation technologies to a mix of renewable and nuclear capacities. Each scenario is detailed with the assumptions in the report, but the dataset used to conduct the study is not open-access. The open-source power system model, Antares [32, 33], describes the production capacities, the network, and the sources of consumption in all European countries, to simulate the production, consumption, and exchanges per country at hourly intervals in all the countries of the European Union. However, the report does not include a sensitivity analysis of the input parameters of the scenarios, and the Antares model uses a cost optimization approach.

The studies [23, 21] analyze the Belgian energy system in 2035 and 2050, respectively, for different GHG emissions targets using the multi-sectors open-source model EnergyScope TD [2]. They optimize the design of the overall system to minimize its costs and emissions. The input data of the model are open-access on the Github repository. A sensitivity analysis is conducted in Rixhon et al. [21] by implementing the PCE approach to emphasize the influence of the parameters on the total cost of the system. They point out Belgium's lack of endogenous renewable resources to achieve ambitious GHG emissions targets. Thus, additional potentials shall be obtained by importing renewable fuels, electricity or deploying geothermal energy.

## Appendix B. FEC calculation

This appendix provides the details to derive the FEC from the simulation results to be used to calculate the system EROI following (1).

The set of end-use demands EUD comprises: (1) electricity; (2) heat: heat high temperature, heat low-temperature DEC, and heat low-temperature DHN; (3) non-energy: ammonia, HVC, and methanol; (4) mobility: freight boat, freight rail, freight road, passenger private, and public. The end-use demand is expressed in [Mpkm/y] (millions of passenger-km) for passenger mobility, [Mtkm/y] (millions of ton-km) for freight mobility, [GWh/y] for heating, [GWh/y] for non-energy, and [GWhe/y] for electricity end-uses.

The system FEC is the sum of the final energy consumption related to each end-use demand (eud):

$$\text{FEC} = \sum_{eud \in \text{EUD}} \text{FEC}(eud). \quad (\text{B.1})$$

Then, for a given end-use demand (eud) the energy balance is

$$eud + \sum_{i \in I} c_i(eud) = \sum_{j \in J} p_j(eud), \quad (\text{B.2})$$

with  $c_i(eud)$  the consumption of this end-use demand by technology  $i$ , and  $p_j(eud)$  the production of this end-use demand by technology  $j$ . For instance, several technologies can produce heat at high temperatures, such as gas boilers or CHP. Furthermore, some technologies use heat at high temperatures as input material, such as technology to produce HVC.

First, let us consider the case where no technology uses this end-use demand as input material:  $I = \emptyset$ . Then, from (B.2) the FEC related to this end-use demand is

$$\text{FEC}(eud) = \sum_{j \in J} \text{FEC}_j(eud). \quad (\text{B.3})$$

If  $j$  is a technology, it produces  $p_j(eud)$  and possibly other outputs, such as electricity or hydrogen, by consuming gas, electricity, or biomass. Then,  $\text{FEC}_j(eud)$  is defined as follows

$$\text{FEC}_j(eud) = \frac{p_j(eud)}{p_j(eud) + \sum \text{outputs}^j} \sum \text{inputs}^j. \quad (\text{B.4})$$

For instance, in the model, when considering the heat high-temperature end-use demand, the technology gas CHP industry consumes 2.1739 GWh of gas to produce 1 GWh of heat high-temperature and 0.9565 GWh of electricity. In this case, the FEC of gas of this technology to produce 1 GWh of heat at high-temperature is

$$\text{FEC} = \frac{1}{1 + 0.9565} 2.1739 \approx 1.111. \quad (\text{B.5})$$

If  $j$  is a resource such as methanol or ammonia, then

$$\text{FEC}_j(eud) = p_j(eud). \quad (\text{B.6})$$

For instance, the methanol end-use demand can be partially satisfied with imports.

Let us consider the case where at least one technology uses this end-use demand as input material:  $I \neq \emptyset$ . Then, the consumptions  $c_i(eud)$  are taken into account as follows to estimate the FEC correctly

$$\tilde{p}_j(eud) = p_j(eud) - \sum_{i \in I} c_i(eud) \frac{p_j(eud)}{\sum_{j \in J} p_j(eud)}. \quad (\text{B.7})$$

Finally, the different  $\text{FEC}_j(eud)$  are estimated as previously described by replacing  $p_j(eud)$  in (B.4) and (B.6) by  $\tilde{p}_j(eud)$  defined in (B.7).

## Appendix C. Reference scenario additional results

This appendix presents the results of the simulation with the reference scenario (see Section 4.1) in terms of installed capacities for several GHG emissions targets, energy invested, and FEC.

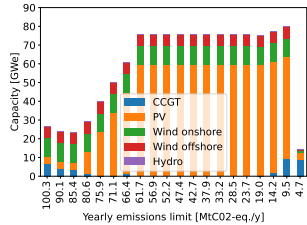
### Appendix C.1. Assets installed capacity evolution

Figure C.13 depicts the installed capacities of electricity production, storage (electric, thermal, gas, ammonia, and methanol), and renewable fuels technologies. The PV technology drives the evolution of electricity production assets by replacing the CCGTs and reaching the maximal available capacity of 59.2 [GWe]. Notice that the onshore and offshore wind technologies are already at their maximal capacities in the “reference scenario-100%”. When the GHG emissions are below 9.5 [MtCO<sub>2</sub>-eq./y], the PV and wind capacities are replaced mainly by CCGT, which uses renewable gas (gas-RE). The electric storage is composed of daily storage: pumped hydro storage<sup>9</sup> (PHS) and batteries of electric vehicle (BEV). The PHS is already at its maximal available capacity in the “reference scenario-100%”, and the batteries of electric vehicles are used when GHG emissions are below 66.4 [MtCO<sub>2</sub>-eq./y] to cope with uncertainty related to the increasing share of PV and wind power in the primary energy mix. With the shift from thermal to electric cars, batteries (BEV) can interact with the electricity layer (vehicle-to-grid) when GHG emissions decrease. They provide additional flexibility to cope with a primary energy mix that relies on an increasing share of intermittent renewable energy as the GHG emissions decrease. Then, when the GHG emissions are below 9.5 [MtCO<sub>2</sub>-eq./y], electric cars are replaced by thermal cars, which use renewable fuels (gas-RE). When the GHG emissions target is below 66.4 [MtCO<sub>2</sub>-eq./y], the PV installed capacity is maximal (59.2 [GWe]), and the system relies on a high share of intermittent renewable energy: solar and wind to produce electricity. The DHN and DEC low heat temperature demands are mainly satisfied by heat pumps. Therefore, the system uses an increased capacity of seasonal thermal DHN and daily thermal DEC storage technologies to cope with the seasonal and daily intermittent electricity production. When the GHG emissions target is below 9.5 [MtCO<sub>2</sub>-eq./y], the primary energy mix comprises renewable fuels, including renewable gas. Thus, the gas boiler technology mainly satisfies the DHN and DEC low heat temperature demands, and the capacities of DHN and daily thermal DEC storage technologies are close to 0 [GWh]. The seasonal gas storage is filled with NG in the “reference scenario-100%”. Its capacity decreases when GHG emissions are  $\approx 85.4$  [MtCO<sub>2</sub>-eq./y] with the electrification of the private mobility. Then, its capacity

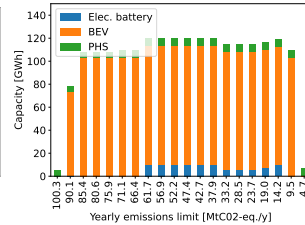
increases when GHG emissions are  $\approx 71.1$  [MtCO<sub>2</sub>-eq./y] and reaches a constant value with GHG emissions from 61.7 to 33.2 [MtCO<sub>2</sub>-eq./y]. Finally, its capacity increases progressively when GHG emissions decrease below 33.2 [MtCO<sub>2</sub>-eq./y] to satisfy the seasonality of the heating, mobility, and electricity demands that rely heavily on renewable gas. The HVC end-use demand, which amounts to most non-energy demand, is satisfied with technology that converts methanol into HVC. The methanol is imported and synthesized from biomass when the GHG emissions are between 100.3 - 33.2 [MtCO<sub>2</sub>-eq./y]. When the GHG emissions are between 33.2 and 9.5 [MtCO<sub>2</sub>-eq./y], the methanol imports are replaced by technologies to synthesize methanol from imported renewable gas. Finally, when the GHG emissions are below 9.5 [MtCO<sub>2</sub>-eq./y], there are only renewable methanol imports.

Figure C.14 depicts the installed capacities of heating and mobility technologies. The industrial gas boilers are replaced by waste boilers and electrical resistors (I elec.) when GHG emissions reach 66.4 [MtCO<sub>2</sub>-eq./y]. It corresponds to the shift from a primary energy mix composed mainly of NG to less intensive carbon energies, such as solar, wind, and waste, to satisfy the heat high-temperature end-use demand. When the GHG emissions are below 14.2 [MtCO<sub>2</sub>-eq./y], the waste boilers are replaced by gas boilers that use renewable fuels, including imported renewable gas. Finally, when the GHG emissions are below 9.5 [MtCO<sub>2</sub>-eq./y], the gas boiler technology is exclusively used with imported renewable gas. The low heat temperature DEC end-use demand is always satisfied with heat pumps, except when GHG emissions decrease below 9.5 [MtCO<sub>2</sub>-eq./y]. In this case, DEC gas boilers are used with imported renewable gas. Overall, the DHN heat low-temperature demand is mainly satisfied with DHN electricity heat pumps when GHG emissions are  $> 14.2$  [MtCO<sub>2</sub>-eq./y]. The decrease of DHN gas CHP is first balanced by DHN electricity heat pumps and then by DHN biomass CHP. When GHG emissions target is below 9.5 [MtCO<sub>2</sub>-eq./y], DHN gas CHP, and gas boiler technologies use imported renewable gas to satisfy the demand. Private mobility relies on electric cars from GHG emissions of 85.4 to 9.5 [MtCO<sub>2</sub>-eq./y] and gas cars using imported renewable gas when GHG emissions decrease below 9.5 [MtCO<sub>2</sub>-eq./y]. The trend is similar for freight trucks. The freight boat first uses NG and then renewable gas when GHG emissions decrease. The freight trains rely only on electricity in EnergyScope TD; thus, there is no technology change for this mobility type.

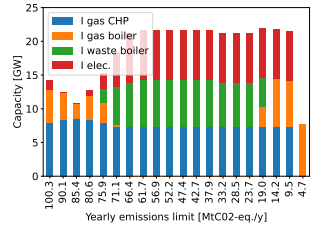
<sup>9</sup>In Belgium, it is mainly the Coo-Trois-Ponts hydroelectric power station.



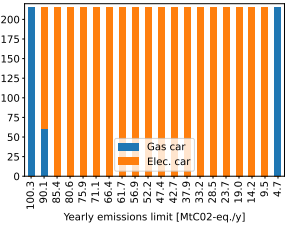
(a) Electricity production.



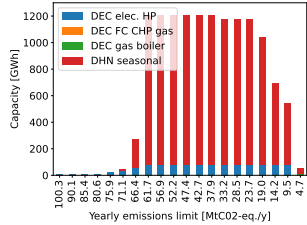
(b) Electric storage.



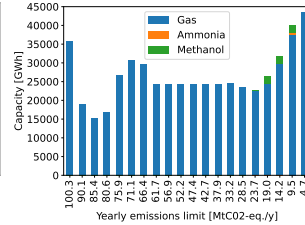
(a) Heat high T.



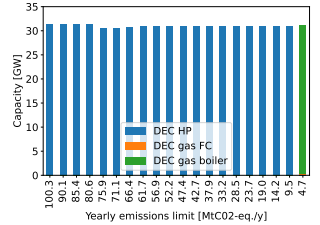
(b) Private mobility.



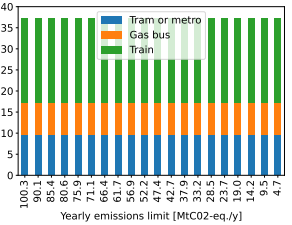
(c) Thermal storage.



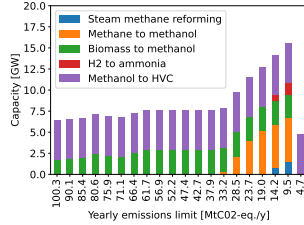
(d) Other storage.



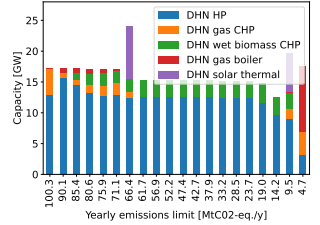
(a) Heat low T DEC.



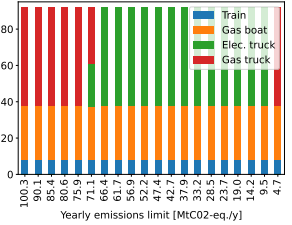
(b) Public mobility.



(e) Renewable fuels.



(c) Heat low T DHN.



(d) Freight mobility.

Figure C.13: Evolution of the electricity production, storage (electric, thermal, gas, ammonia, and methanol), and renewable fuels asset installed capacities breakdown by technology for several scenarios of GHG emissions in 2035. Abbreviations: combined cycle gas turbine (CCGT), photovoltaic (PV), electric (elec.), battery of electric vehicle (BEV), pumped hydro storage (PHS), decentralized (DEC), district heating networks (DHN), fuel cell (FC), combined heat and power (CHP), heat pump (HP), high value chemicals (HVC).

## Appendix C.2. Energy invested evolution

Figures C.15 and C.16 depict the operation ( $E_{op}$ ) and construction ( $E_{constr}$ ) system energy invested breakdown by resources, between renewable and non-renewable, and technologies (all technologies, and between electricity and mobility technologies).

The total system energy invested ( $E_{in,tot}$ ) increases with the limitation of GHG emissions due to the increase of  $E_{constr}$  and  $E_{op}$ , and is driven by the increase of renewable fuels. The  $E_{op}$  increase is mainly due to the shift from NG to renewable gas, and it exceeds the construction system energy invested when GHG emissions are below 47.4 [MtCO<sub>2</sub>-eq./y]. The main drivers of the  $E_{constr}$  increase are the PV technology and the shift from NG cars and trucks to electric cars and trucks.

Figure C.14: Evolution of the heat and mobility asset installed capacities breakdown by technology for several scenarios of GHG emissions in 2035. Abbreviations: industry (I), combined heat and power (CHP), decentralized (DEC), district heating networks (DHN), electric (elec.), heat pump (HP), fuel cell (FC).

## Appendix C.3. FEC evolution

Figure C.17 depicts the evolution of the FEC breakdown by end-use demand: heat, mobility, non-energy, and electricity. First, the FEC decreases with the shift from NG cars to better efficient electric cars. Then, it increases slightly due to the shift from DHN gas co-generation to DHN bio hydrolysis CHP technology that uses more primary energy to produce the same amount of heat low-temperature end-use demand. Finally, it decreases with the shift from NG trucks to more efficient electric trucks. When GHG emissions achieve 4.7 [MtCO<sub>2</sub>-eq./y], the heat low-temperature decentralized FEC increases with the shift from electric technologies such as heat pumps to gas boilers that use renewable gas. Then, the FEC of mobility, public and freight road, increases due to the shift from electric vehicles to renewable fuel vehicles.

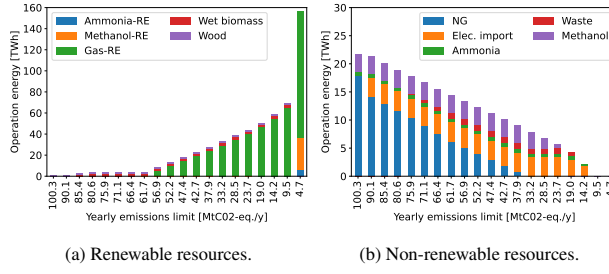


Figure C.15: System energy invested in operation ( $E_{op}$ ) evolution in 2035 for several GHG emissions targets breakdown between renewable (left) and non-renewable resources (right). Abbreviations: RE-fuels: gas-RE, methanol-RE, and ammonia-RE; electricity (Elec.).

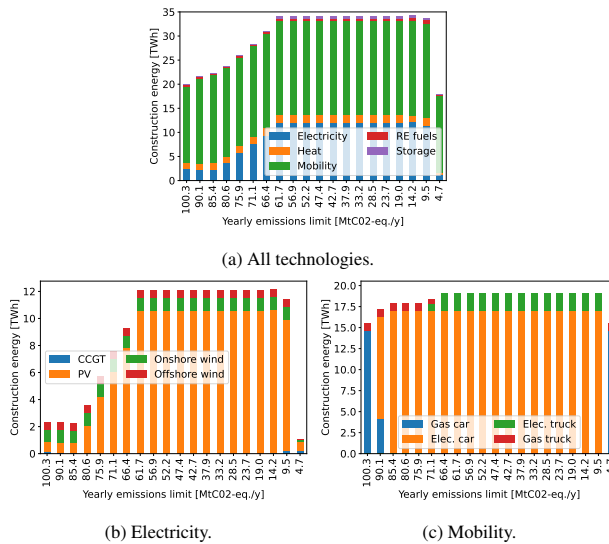


Figure C.16: System energy invested in construction ( $E_{constr}$ ) evolution in 2035 for several GHG emissions targets (upper), and breakdown between electricity (lower left) and mobility (lower right) technologies. Abbreviations: RE-fuels: gas-RE, methanol-RE, and ammonia-RE; natural gas (NG); electric (Elec.).

## Appendix D. Sensitivity analysis

This appendix details the sensitivity analysis methodology and provides additional results. Figure D.18 depicts the framework of the EROI system sensitivity analysis and how the PCE method is implemented. First, uncertain parameters are defined with their respective uncertainty ranges. Then, the PCE framework is applied to generate a surrogate model and retrieve the critical uncertain parameters. Finally, the mean and variance of the system EROI are estimated, and the surrogate model is used to perform Monte Carlo sampling to estimate the EROI pdf for several GHG emissions targets.

This appendix is organized as follows. First, Appendix D.1 details the framework used to perform

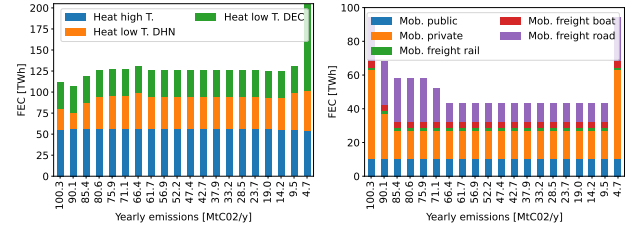


Figure C.17: Final energy consumption (FEC) evolution for several GHG emissions targets in 2035 breakdown by end use demand: heat (upper left), mobility (upper right), non-energy and electricity (lower). Abbreviations: temperature (T.); district heating networks (DHN), de-centralized (DEC); mobility (Mob.); high value chemicals (HVC).

the sensitivity analysis of the system EROI. Then, Appendix D.2 presents the set of uncertain parameters considered with their respective uncertainty ranges. Finally, Appendix D.3 illustrates the selection process using the first-order PCE to build a shortlist of uncertain parameters for the second-order PCE.

### Appendix D.1. Sensitivity analysis methodology

The PCE approach provides a computationally efficient alternative to the Monte Carlo simulation for uncertainty quantification to address the “curse of dimensionality” pointed out by Rixhon et al. [21]. Indeed, given limited information about the uncertainty of the parameters for long-term energy planning models, the PCE method constructs a series of multivariate orthonormal polynomials used as a surrogate model  $\hat{f}$ . It is a closed-form function that takes as input a vector composed of the values of the realization  $i$  of the  $N$  uncertain parameters considered  $\underline{X}^i = [X_1^i, \dots, X_n^i]^T$  and outputs the system EROI

$$\hat{f}(\underline{X}^i) = \text{EROI}^i. \quad (\text{D.1})$$

Depending on the number of uncertain parameters, the polynomial order can be increased and is, therefore, more accurate. A few hundred evaluations are required for tens of uncertain parameters to have a first-order polynomial. However, thousands of evaluations are required to obtain a third-order polynomial. Then, the

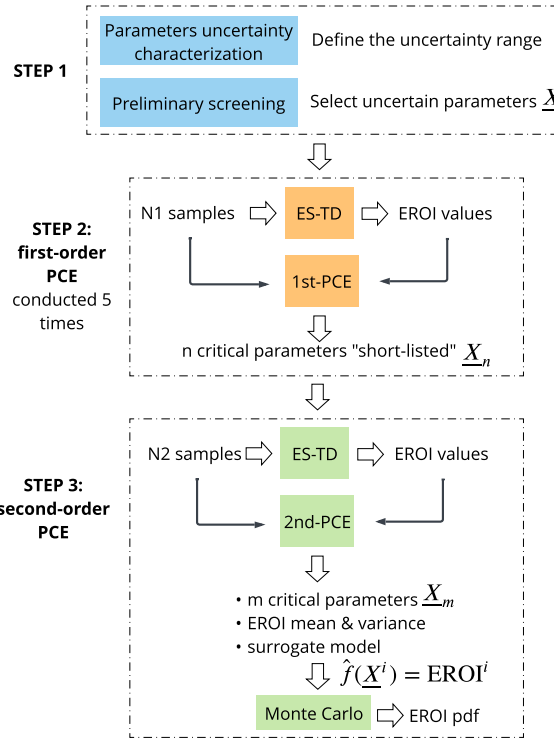


Figure D.18: Framework of the EROI system sensitivity analysis. The steps 2 and 3 are conducted for each GHG emissions target considered.

surrogate model (D.1) allows: (1) to extract statistical moments such as the mean and variance using the coefficients and the total-order Sobol indices. They illustrate the contribution of each uncertain input parameter to the variance of the quantity of interest, in our case, the system EROI, including the mutual interactions; (2) to conduct a Monte-Carlo evaluation where millions of samples are generated, and the associated results are calculated instantaneously. It provides the accurate estimation of the system EROI pdf for several GHG emissions targets.

The first step, depicted in Figure D.18, is the uncertainty characterization which consists of defining a set of uncertain parameters and their uncertainty ranges. In this study, we use the extension to the Belgian energy system uncertainty characterization performed by Limpens [46] based on the work of Moret et al. [51]. A preliminary screening was performed to determine which parameters had no impact and resulted in a set of 138 uncertain parameters  $\underline{X}_0 = [X_1, \dots, X_{138}]^\top$ . The second step consists of conducting a first-order PCE on these 138 uncertain parameters to build a shortlist of  $n$  critical parameters  $\underline{X}_n$  used for a second-order PCE.

This step is performed five times to increase the confidence of the result. A parameter is considered negligible if its total-order Sobol index is close to 0 for all five cases. The last step consists of conducting a second-order PCE to identify the  $m$  critical uncertain parameters  $\underline{X}_m$  based on  $\underline{X}_n$  and estimating an accurate total-order Sobol index for each of them. Then, a Monte-Carlo evaluation is performed using the surrogate model  $\hat{f}$  to estimate the pdf of the system EROI for several GHG emissions targets. Steps 2 and 3 are conducted for each several GHG emissions targets.

#### Appendix D.2. Uncertainty characterization

Accounting for uncertainties in energy system long-term planning is crucial [55] to obtain robust designs against uncertainty. However, the insufficient quantity and quality of available data is frequently a limitation. This challenge is addressed in Moret et al. [51] by developing an application-driven method for uncertainty characterization, allowing the definition of ranges of variation for the uncertain parameters. These ranges were initially defined for the Swiss energy system and have been adapted for Belgium [46, 21]. Similarly, this study assumes that all the uncertain parameters are independent and uniformly distributed between their lower and upper bounds.

Table D.9 summarizes the uncertainty ranges for the different groups of technologies and resources considered in the sensitivity analysis. Following the approach developed by Moret et al. [51] and capitalizing on the works of Limpens [46], Rixhon et al. [21] the uncertainty intervals are defined. A preliminary screening, including all the parameters of the model, allowed to obtain an initial list of 138 parameters to be used for the first-order PCE.

There are four categories of uncertain parameters: end-use demands, technologies, resources, and others. The uncertainty in the yearly end-use demands is split by energy sectors. The electricity demand, space heating demand, and industrial demand are related to the yearly industrial demand uncertainty  $\text{endUses}_{\text{year}}^I$ , which has the most extensive range. The freight and passenger mobility are related to the uncertainty of transport  $\text{endUses}_{\text{year}}^{TR}$ . Technologies are defined through different parameters: the energy conversion efficiency  $\eta$ , the investment cost  $c_{\text{inv}}$ , the construction energy investment  $e_{\text{constr}}$ , the yearly  $c_p$  and hourly  $c_{p,t}$  load factors, the potential  $f_{\text{max}}$ , the maintenance cost  $c_{\text{maint}}$ , and the lifetime. This study does not consider the energy conversion efficiency, investment and maintenance costs, yearly capacity factors, and lifetime as uncertain parameters. In addition, the energy invested in the construc-

Category	rep. param.	min	max
$\text{endUses}_{\text{year}}^I$	$\text{endUses}_{\text{year}}^I$	-10.5%	+5.9%
$\text{endUses}_{\text{year}}^{\text{TR}}$	$\text{endUses}_{\text{year}}^{\text{TR}}$	-3.4%	+3.4%
$\text{avail}$	$\text{avail}^{\text{Waste}}$	-32.1%	+32.1%
$f_{\max}$	$f_{\max}^{\text{PV}}$	-24.1%	+24.1%
$c_{p,t}$	$c_{p,t}^{\text{PV}}$	-11.1%	+11.1%
$\%_{\text{loss}}$	$\%_{\text{loss}}^{\text{elec}}$	-2%	+2%
$e_{\text{constr}}$	$e_{\text{constr}}^{\text{cars}}$	-25%	+25%
$e_{\text{op}}$	$e_{\text{op}}^{\text{RE-fuels}}$	-25%	+25%
<i>Others</i>	$f_{\max}^{\text{NUC}}$	0.0	5.6
	$f_{\max}^{\text{GEO elec}}$	0.0	2.0
	$f_{\max}^{\text{GEO DHN}}$	0.0	2.0
	$\%_{\max}^{\text{public mob}}$	45.0%	55.0%
	$\%_{\max}^{\text{train freight}}$	22.5%	27.5%
	$\%_{\max}^{\text{boat freight}}$	27.0%	33.0%
	$\%_{\max}^{\text{DHN heat}}$	33.3%	40.7%
	$e_{\text{elec}}_{\text{max}}^{\text{import}}$	8,749	10,692

Table D.9: Application of the uncertainty characterization method [51] to EnergyScope TD when maximizing the system EROI. Uncertainty is characterized for one representative parameter (rep. param.) per category. Due to the lack of data in the literature for 2035, the uncertainty intervals of  $e_{\text{op}}$  and  $e_{\text{constr}}$  are by default absolute uniform interval  $\text{UI}[-25\%, +25\%]$ . Abbreviations: photovoltaic (PV), district heating network (DHN), industry (I), transport (TR), nuclear (NUC), geothermal (GEO), electricity (elec).

tion of storage technologies is not taken into account. Intermittent renewable energy is limited in its potential ( $f_{\max}$  of PV, onshore and offshore wind) and the hourly capacity factor ( $c_{p,t}$  of PV, solar, onshore and offshore wind, and hydroelectricity). The electricity  $\%_{\text{loss}}^{\text{elec}}$  and heat  $\%_{\text{loss}}^{\text{heat}}$  network losses are considered uncertain parameters. Resources are characterized by an operating cost  $c_{\text{op}}$ , not considered uncertain in this study, energy invested in operation  $e_{\text{op}}$ , and availability  $\text{avail}$ . Most resources have unlimited availability except biomass, waste, and electricity imported. The availability of local resources (wood, waste, and biomass) are uncertain parameters. Finally, there is a limited installed capacity  $f_{\max}$  imposed arbitrarily for nuclear  $f_{\max}^{\text{NUC}}$  [GWe], electricity  $f_{\max}^{\text{GEO elec}}$  [GWe] and heat  $f_{\max}^{\text{GEO DHN}}$  [GWth] production from geothermal. This work also accounts for uncertainties on the upper bounds of mobility  $\%_{\max}^{\text{public mob}}$  [%],  $\%_{\max}^{\text{train freight}}$  [%] and  $\%_{\max}^{\text{boat freight}}$  [%], the upper bound of heat that can be covered by district heating network  $\%_{\max}^{\text{DHN heat}}$ , and the capacity of electrical interconnection with neighbours  $e_{\text{elec}}_{\text{max}}^{\text{import}}$  [GWe].

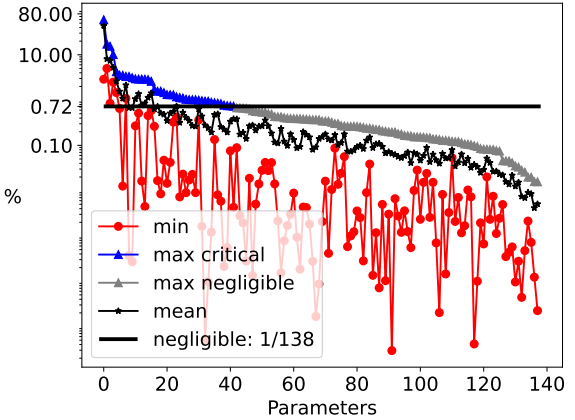


Figure D.19: Illustration of the selection process using first-order PCE for  $\text{GWP}_{\text{to}} \leq 28.5$  [MtCO<sub>2</sub>-eq./y]. The y-axis is logarithmic. For each parameter, the blue mark indicates the parameter is critical, and the grey mark that it is negligible. It corresponds to the maximal value of the Sobol index over the five runs. A parameter is critical if its maximal value of the Sobol index over the five runs is above threshold =  $1/d$ . The red (black) mark is the minimum (mean) value of the Sobol index over the five runs.

#### Appendix D.3. First-order PCE results

The second step, depicted in Figure D.18, consists of using the first-order PCE to build shorter lists of uncertain parameters for the second-order PCE. This selection is performed for each GHG emissions target considered in the sensitivity analysis. It relies on good practice [56], by selecting the parameters which have at least, over the five runs, *i.e.*, to ensure redundancy, one total-order Sobol index above the threshold =  $1/d$ , where  $d = 138$  is the number of uncertain parameters at the pre-selection phase. These parameters short-listed are named critical parameters and considered for the rest of the study in the second-order PCE.

Figure D.19 illustrates this selection process using the first-order PCE for the GHG emissions target of 28.5 [MtCO<sub>2</sub>-eq./y]. In this scenario, 42 parameters are identified (blue marks) as critical to be used in the second-order PCE. The red marks are the minimum values of the Sobol index for each parameter over the five runs, and the black marks are the mean of their five Sobol index values.

#### Appendix D.4. Second-order PCE results

The final step, depicted in Figure D.18, consists of using the second-order PCE on the parameters short-listed to limit the error below 1% [53] on the EROI statistical moments: mean  $\mu$  and variance  $\sigma$ .

GHG target [MtCO <sub>2</sub> -eq./y]	85.4	56.9	28.5	19.0
# parameters short-listed	64	55	42	45
# critical parameters	9	27	17	5

Table D.10: Number (#) of short-listed and critical parameters using the first-order and second-order PCE.

Figure D.20 depicts the selection of the critical parameters using the second-order PCE for the GHG emissions targets considered. Table D.10 presents the number (#) of short-listed and critical parameters using the first-order and second-order PCE. Finally, Table D.11 lists the critical parameters and their Sobol index for the GHG emissions targets considered.

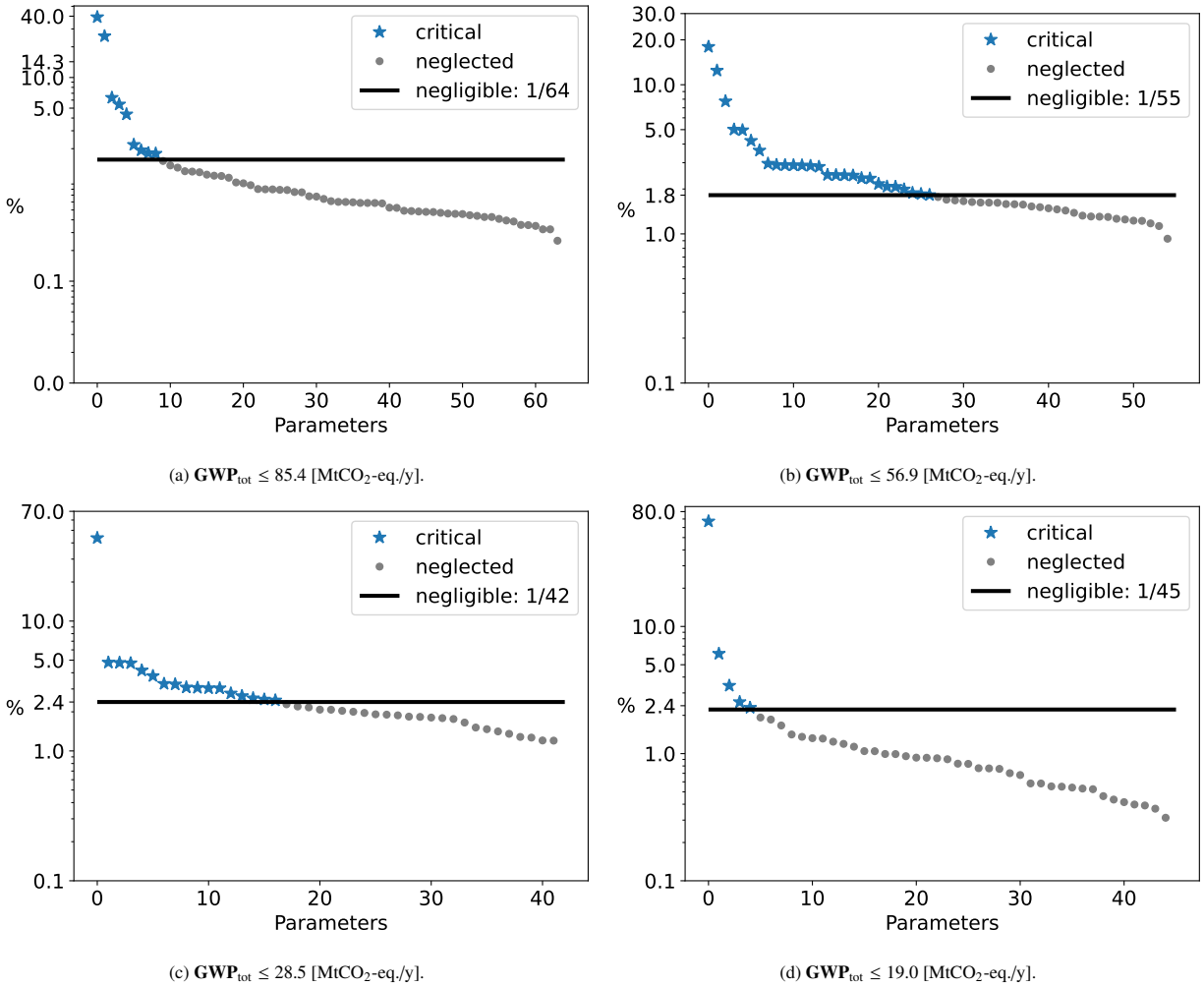


Figure D.20: Sobol indices of the parameters using the second-order PCE. Parameters are sorted and critical ones (in blue) have an index above the threshold  $1/d$ , with  $d$  the number of uncertain parameters considered in the second-order PCE. The y-axis is logarithmic.

Ranking	85.4	56.9	28.5	19.0
1	$e_{\text{constr}}^{\text{NG cars}}$ 39.2	$e_{\text{constr}}^{\text{Elec. cars}}$ 18.0	$e_{\text{op}}^{\text{Gas-RE}}$ 43.6	$e_{\text{op}}^{\text{Gas-RE}}$ 67.1
2	$e_{\text{op}}^{\text{NG}}$ 25.5	$f_{\text{max}}^{\text{NUC}}$ 12.5	$e_{\text{constr}}^{\text{Elec. cars}}$ 4.8	$e_{\text{constr}}^{\text{Elec. cars}}$ 6.1
3	$e_{\text{constr}}^{\text{Elec. cars}}$ 6.3	$\%_{\text{max}}^{\text{public mob}}$ 7.7	$f_{\text{max}}^{\text{NUC}}$ 4.8	$f_{\text{max}}^{\text{NUC}}$ 3.4
4	$\%_{\text{max}}^{\text{public mob}}$ 5.4	$e_{\text{constr}}^{\text{PV}}$ 5.0	$\text{avail}^{\text{Wet biomass}}$ 4.7	$\text{avail}^{\text{Wood}}$ 2.5
5	$e_{\text{op}}^{\text{Wet biomass}}$ 4.3	$e_{\text{op}}^{\text{NG}}$ 5.0	$f_{\text{max}}^{\text{Offshore wind}}$ 4.2	$e_{\text{constr}}^{\text{NG cars}}$ 2.3
6	$e_{\text{constr}}^{\text{DHN wet biomass CHP}}$ 2.2	$\text{avail}^{\text{Wood}}$ 4.2	$\text{endUses}^{\text{I}}_{\text{year}}$ 3.8	-
7	$e_{\text{constr}}^{\text{Elec. trucks}}$ 1.9	$e_{\text{constr}}^{\text{NG cars}}$ 3.6	$f_{\text{max}}^{\text{GEO DHN}}$ 3.3	-
8	$e_{\text{op}}^{\text{Methanol}}$ 1.8	$c_{p,t}^{\text{PV}}$ 3.0	$e_{\text{constr}}^{\text{PV}}$ 3.3	-
9	$e_{\text{constr}}^{\text{Diesel trucks}}$ 1.8	$\text{endUses}^{\text{I}}_{\text{year}}$ 3.9	$e_{\text{constr}}^{\text{Offshore wind}}$ 3.1	-
10	-	$e_{\text{op}}^{\text{Uranium}}$ 2.9	$\%_{\text{max}}^{\text{public mob}}$ 3.1	-
11	-	$\text{avail}^{\text{Wet biomass}}$ 2.9	$f_{\text{max}}^{\text{Onshore wind}}$ 3.0	-
12	-	$f_{\text{max}}^{\text{GEO DHN}}$ 2.9	$e_{\text{constr}}^{\text{NG cars}}$ 3.0	-
13	-	$e_{\text{op}}^{\text{Wet biomass}}$ 2.9	$e_{\text{op}}^{\text{Elec.}}$ 2.8	-
14	-	$e_{\text{op}}^{\text{Gas-RE}}$ 2.8	$\text{avail}^{\text{Wood}}$ 2.6	-
15	-	$c_{p,t}^{\text{Offshore wind}}$ 2.5	$e_{\text{op}}^{\text{Wet biomass}}$ 2.5	-
16	-	$f_{\text{max}}^{\text{Offshore wind}}$ 2.5	$e_{\text{constr}}^{\text{Elec. wet biomass}}$ 2.5	-
17	-	$e_{\text{op}}^{\text{Methanol}}$ 2.5	$c_{p,t}^{\text{Offshore wind}}$ 2.5	-
18	-	$f_{\text{max}}^{\text{Onshore wind}}$ 2.5	-	-
19	-	$\text{endUses}^{\text{TR}}_{\text{year}}$ 2.4	-	-
20	-	$e_{\text{constr}}^{\text{H2}}$ 2.4	-	-
21	-	$\%_{\text{max}}^{\text{freight train}}$ 2.2	-	-
22	-	$c_{p,t}^{\text{Onshore wind}}$ 2.1	-	-
23	-	$\%_{\text{max}}^{\text{freight boat}}$ 2.1	-	-
24	-	$e_{\text{constr}}^{\text{I waste boilers}}$ 2.0	-	-
25	-	$e_{\text{constr}}^{\text{DHN waste CHP}}$ 1.9	-	-
26	-	$e_{\text{op}}^{\text{Wood}}$ 1.8	-	-
27	-	$e_{\text{constr}}^{\text{CCGT ammonia}}$ 1.8	-	-

Table D.11: Critical parameters and Sobol indices values [%] for several GHG emissions targets [MtCO<sub>2</sub>-eq./y]. Abbreviations: electric (elec.), mobility (mob), photovoltaic (PV), nuclear (NUC), renewable gas (Gas-RE), natural gas (NG), geothermal (GEO), transport (TR), industry (I), district heating networks (DHN), combined heat and power (CHP), combined cycle gas turbine (CCGT).